DGfM

ORIGINAL ARTICLE

Pyrenochaeta fraxinina as colonizer of ash and sycamore petioles, its morphology, ecology, and phylogenetic connections

P. Bilański[1] · B. Grad[1] · T. Kowalski[1]

Abstract

Pyrenochaeta fraxinina was first described in 1913 from the state of New York (USA) on petioles of *Fraxinus* sp. Since then, the species has not been reported from North America and reports from the other regions of the world are very sparse. The results of this study on *P. fraxinina* are based on the material collected in various regions of Poland from 2012 to 2019. The material comprised 2700 previous year's leaf petioles of *Fraxinus excelsior* and 1970 petioles or leaf residues of eight other deciduous tree species. As a result, the occurrence of pycnidial conidiomata of *P. fraxinina* was confirmed on *F. excelsior* (3.4% of petioles), *F. mandshurica* (1.5%), *F. pennsylvanica* (3.2%), and *Acer pseudoplatanus* (2.0%). The morphology of the microstructures was described based on the fresh material and compared with the holotype of *P. fraxinina*. The optimal temperature for the growth of the fungus in vitro was estimated as 20 °C. The analyses based on ITS-LSU rDNA sequences and a protein coding sequence of *TUB2* and *RPB2* genes showed that *P. fraxinina* isolates form a well-supported clade in the phylogenetic trees. The species proved to be closely related to *Nematostoma parasiticum* (asexual morph *Pyrenochaeta parasitica*), a species occurring on *Abies alba* in connection with needle browning disease. Interactions between *P. fraxinina* and the ash dieback pathogen, *Hymenoscyphus fraxineus*, were analyzed in vivo on ash petioles and in vitro in dual cultures. Among 93 petioles of *F. excelsior*, for which *P. fraxinina* conidiomata were detected, 26 were also colonized by *H. fraxineus*. Mostly, these two fungi occurred separately, colonizing different sections of a petiole. For all dual cultures, both fungi, *P. fraxinina* and *H. fraxineus*, showed growth inhibition toward the counterpartner. The role of *P. fraxinina* as a saprotrophic competitor toward *H. fraxineus* in ash petioles is discussed.

Keywords *Acer* · Ash dieback · Competition · *Fraxinus* · *Hymenoscyphus fraxineus* · *Nematostoma parasiticum*

Introduction

The ascomycete genus *Pyrenochaeta*, with 118 currently accepted species, belong to order *Pleosporales*, class *Dothideomycetes* (de Gruyter et al. 2010; Wijayawardene et al. 2012; Index Fungorum 2022). It was introduced by De Notaris (1849) with *Pyrenochaeta nobilis* De Not as the type species. The genus is characterized by simple, setose, unilocular, ostiolate pycnidial conidiomata, elongated, filiform, branched, multiseptate, acropleurogenous conidiophores and hyaline, unicellular conidia (De Notaris 1849; Schneider 1979; Sutton 1980; de Gruyter et al. 2010; Wanasinghe et al. 2017). For most of the species within the genus, only asexual stages are known (no sexual morph connections established). Some *Pyrenochaeta* or pyrenochaeta-like species, however, have been reported as anamorphs for the following ascomycetous genera: *Byssosphaeria*, *Cucurbitaria*, *Herpotrichia*, *Keissleriella*, *Nematostoma*, *Neopeckia* (Schneider 1979; Sutton 1980; Barr 1984, 1997; Sivanesan 1984; Chen and Hsieh 2004; de Gruyter et al. 2010; Zhang et al. 2012; Doilom et al. 2013; Wanasinghe et al. 2017; Jaklitsch et al. 2018; Hongsanan et al. 2020).

The taxonomic position of *Pyrenochaeta* has been a subject of multiple studies, as this genus accommodates more than 160 epithets (Valenzuela-Lopez et al. 2018; Index

---

✉ P. Bilański
piotr.bilanski@urk.edu.pl

T. Kowalski
rltkowal@cyf-kr.edu.pl

[1] Department of Forest Ecosystem Protection, Faculty of Forestry, University of Agriculture in Kraków, Al. 29-Listopada 46, 31–425 Kraków, Poland

Fungorum 2022). As a result, the taxonomy of the genus has undergone major changes in recent years, mainly due to the extensive use of molecular techniques that enabled more natural classification of this group of fungi (Doilom et al. 2013; Jaklitsch et al. 2018; Valenzuela-Lopez et al. 2018). The recent phylogenetic analyses resulted in numerous *Pyrenochaeta* species being transferred to newly described genera, e.g., *Pyrenochaeta cava*, *P. quercina*, and *P. unguis-hominis* have been moved to *Neocucurbitaria*, *P. acicola* to *Neopyrenochaeta*, *P. lycopersici* to *Pseudopyrenochaeta*, and *P. corni* to *Paracucurbitaria* (de Gruyter et al. 2010; Wijayawardene et al. 2012; Zhang et al. 2012; Doilom et al. 2013; Wanasinghe et al. 2017; Jaklitsch et al. 2018; Valenzuela-Lopez et al. 2018).

In the environment, numerous *Pyrenochaeta* species are found as saprotrophs in soil, plant debris, and wood (Schneider 1979; Sutton 1980; Sivanesan 1984; Sieber 1995), but some species have been identified as tree endophytes. Haňáčková et al. (2017a) detected *Pyrenochaeta corni* in live symptomless shoots of *Fraxinus excelsior*, while occurrence of *P. cava* has been recorded in live leaves of *F. excelsior* and *F. ornus* (Ibrahim et al. 2017; Schlegel et al. 2018). Another *Pyrenochaeta* morphotype, similar to *P. unguis-hominis*, has been isolated from *F. excelsior* leaves by Scholtysik et al. (2013). Some of the *Pyrenochaeta* species cause serious plant diseases in agriculture and forestry. *Pyrenochaeta lycopersici* is a cause of corky-root, an important soil-borne disease of tomato and other solanaceous crops worldwide (Grove and Campbell 1987; Infantino et al. 2003). Another soil-borne pathogen, *P. terrestris*, causes pink rot of onion and root rot of maize and other agricultural plants (Biles et al. 1992; Lević et al. 2011; Yang et al. 2017). *Pyrenochaeta rubi-idaei* causes lesions on leaves of *Rubus idaeus* (Schneider 1979; Sutton 1980). *Pyrenochaeta parasitica* occurs on firs in connection with needle browning disease (Freyer and van der Aa 1975; Butin 1995; Kowalski and Andruch 2012). *Herpotrichia juniperi* and *Neopeckia coulteri* (with *Pyrenochaeta* anamorphs) cause shoot and needle diseases of conifers (Barr 1984; Butin 1995; Sinclair and Lyon 2005). *Pyrenochaeta corni* is often found in Europe in association with bacterial canker of ash (Boerema et al. 2004). Moreover, *Pyrenochaeta* species may be involved in infections of humans. *Pyrenochaeta keratinophila* and *P. unguis-hominis* cause skin and nails infection (Verkley et al. 2010; Toh et al. 2016) and *P. romeroi* is one of the agents of black-grain eumycetoma (Ahmed et al. 2014).

Since the early 1990s, European ash forests are heavily damaged by ash dieback, an epidemic disease that seriously threatened the very existence of *F. excelsior* in Europe (Enderle et al. 2019). The disease is caused be an alien invasive ascomycete, *Hymenoscyphus fraxineus* (anamorph *Chalara fraxinea*) (Kowalski 2006; Baral et al. 2014), that likely have originated from Eastern Asia, where it occurs as

endophyte, extensive leaf colonizer, and locally as leaf pathogen of *Fraxinus mandshurica* and *F. rhynchophylla* (Zhao et al. 2013; Baral et al. 2014; Zheng and Zhuang 2014; Cleary et al. 2016; Drenkhan et al. 2017). The fungus produces numerous apothecia on overwintered leaf petioles lying in the litter, which are the main source of infectious material for the pathogen. In the last few years, numerous studies were carried out in Poland concerning fungal community of ash petiole colonizers and their biocontrol potential toward the ash pathogen *H. fraxineus* (Kowalski and Bilański 2021; Bilański and Kowalski 2022). One of the most interesting species detected during these investigations based on morphological features was *Pyrenochaeta fraxinina* Fairm. The species was first described early in the twentieth century from the state of New York (USA) on petioles of *Fraxinus* sp. (Fairman 1913), since then it has not been reported from North America anymore (Farr et al. 1989; Bates et al. 2018). The only other representative of this genus reported from *Fraxinus* sp. in America was not identified to species level (Brambilla and Sutton 1969; Bates et al. 2018). *Pyrenochaeta fraxinina* does not appear on checklists of fungi in many European countries (e.g., Lizoň and Bacigalova 1998; Læssøe et al. 2017; Gargominy 2019). Axenic cultures of the species have not been deposited in any publicly available biological resource centers. There are no DNA barcode data on the species in the GenBank as well. Thus, although members of *Pyrenochaeta* are a subject of numerous recent phylogenetic reconstructions, *P. fraxinina* has not been included in these analyses (Schoch et al. 2006; de Gruyter et al. 2010, 2013; Hyde et al. 2011; Zhang et al. 2012; Doilom et al. 2013; Wanasinghe et al. 2017; Jaklitsch et al. 2018; Valenzuela-Lopez et al. 2018).

Thus, the aims of this study were (i) ascertainment of the frequency of *P. fraxinina* occurrence on *F. excelsior* petioles, and determination whether the host spectrum for the fungus includes also other tree species; (ii) characterization of *P. fraxinina* colonies, description of the morphology of fruiting bodies, and comparison with original (holotype) description; (iii) determination of the phylogenetic position of *P. fraxinina* in relation to other *Pyrenochaeta* spp. and to other related species; and (iv) investigation of the interactions between *P. fraxinina* and the ash pathogen *H. fraxineus* on *F. excelsior* petioles in vivo and in dual cultures.

Materials and methods

Material studied

The primary material in this study comprised overwintered leaf petioles of three ash species: *Fraxinus excelsior*, *F. mandshurica*, and *F. pennsylvanica* collected from the litter. Petioles were sampled with varying frequency from 2012 to 2019 in various regions of Poland

(Table 1, Fig. 1). For this study by using the term "petiole," we refer to the entire main axis of ash leaf including the distal rachis (after Gross and Han 2015).

Fraxinus excelsior petioles were collected in twenty-three 30- to 120-year-old forest stands (Table 1, Fig. 1). These included both monospecific and mixed species stands, in which F. excelsior showed ash decline symptoms. For each stand, 2–6 petioles were collected from 10 random locations (20–60 petioles per stand). Most of the stands were sampled only once, but for six stands the sampling was repeated three to eight times. A total number of 2,700 of F. excelsior leaf petioles collected in various seasons were subjected to mycological analysis (Table 1). Fraxinus mandshurica petioles were collected only at one site located at Rogów Arboretum in Central Poland (Table 1, Fig. 1). Petioles of F. pennsylvanica were collected from 2017 to 2019 at two forest sites in south-western Poland and from an urban greenery area located in Kraków-Zakrzówek (Table 1, Fig. 1). Additional material, represented by 30 to 100 overwintered leaf petioles or another leaf debris of six deciduous tree species, predominantly Acer pseudoplatanus, was collected from the litter in some regions where F. excelsior petioles were sampled (Table 1). The samples from each stand, and for each tree species, were packed separately in plastic bags and brought to the laboratory for analysis. For comparative purposes, microscopic analyses of the holotype Pyrenochaeta fraxinina Fair. (CUP-F. 3368), obtained from The Cornell Plant Pathology Herbarium, Cornell University, Ithaca, USA, were performed.

Culturing and morphological observations

Identification of P. fraxinina was carried out by means of microscopic analysis of the morphology of characteristic fruiting bodies formed on collected petioles. Fungal microstructures were observed and measured mounted in distilled water on microscope slides, while the holotype was analyzed in the 2% KOH solution (Baral 1989). Morphological observations were performed using either a Zeiss V12 Discovery stereomicroscope (Zeiss, Göttingen, Germany) or a Zeiss Axiophot light microscope with differential interference contrast (DIC) illumination or phase contrast. Photomicrographs were taken with AxioCam MRc5 and HR3 digital cameras.

The frequency of P. fraxinina occurrence was estimated as proportion of petioles bearing species' conidiomata to the overall number of analyzed petioles. These data, i.e., the frequencies of conidiomata bearing petioles, were gathered separately for spring and for autumn to determine the primary season of fructification of P. fraxinina on F. excelsior, F. pennsylvanica, and A. pseudoplatanus (Table 1). In addition, for F. excelsior petioles with P. fraxinina pycnidia, the extent of H. fraxineus colonization was determined using the occurrence of typical for this species black pseudosclerotial plate as an indicator (Baral and Bemmann 2014; Gross and Holdenrieder 2013).

Table 1 Numbers of examined leaf petioles and numbers of petioles with observed conidiomata of *Pyrenochaeta fraxinina*

Tree species	Analyzed season*	Sampling year	Number of sampling sites (sites with confirmed occurrence of *P. fraxinina*)	Number of analyzed petioles	Number (%) of petioles with conidiomata
Conidiomata of *P. fraxinina* observed					
Fraxinus excelsior	a	2012–2017	9 (2)	820	2 (0.2)
	b	2012–2019	23 (17)	1880	91 (4.8)
	total		23 (17)	2700	93 (3.4)
Fraxinus mandshurica	b	2015, 2016	1 (1)	200	3 (1.5)
Fraxinus pennsylvanica	a	2017–2019	1 (0)	60	0 (0.0)
	b	2017–2018	3 (3)	320	12 (3.8)
	total		3 (3)	380	12 (3.2)
Acer pseudoplatanus	a	2013–2019	9 (0)	270	0 (0.0)
	b	2013–2017	10 (5)	590	17 (2.9)
	total		10 (5)	860	17 (2.0)
No conidiomata of *P. fraxinina* observed					
Aesculus hippocastanum	b	2014–2016	2 (0)	200	0
Carpinus betulus	b	2018	2 (0)	60	0
Fagus sylvatica	b	2018	2 (0)	100	0
Quercus robur	b	2018	3 (0)	120	0
Quercus rubra	b	2018	1 (0)	50	0

*Petioles analyzed in: April–August (a), September–December (b)

Fig. 1 Locations of sampling sites and occurrence frequency [%] of *Pyrenochaeta fraxinina* on host plants: **a** *Acer pseudoplatanus*, **b** *Fraxinus excelsior*, **c** *F. mandshurica*, **d** *F. pennsylvanica*. Full-colored markers indicate the occurrence and outline markers the lack of occurrence of *P. fraxinina*. Localities: 1 Stara Hańcza, 2 Szeszupka, 3 Mikołajki, 4 Miłomłyn, 5 Trzęsacz, 6 Kowary, 7 Jelcz, 8 Bystrzyca, 9 Rogów, 10 Puławy, 11 Jędrzejów, 12 Świerklaniec, 13 Prudnik, 14 Rybnik, 15 Dubie, 16 Ojców, 17 Miechów – Domiarki, 18 Kraków – Zakrzówek, 19 Brody, 20 Myślenice, 21 Konina, 22 Przysietnica, 23 Krynica Górska, 24 Dynów, 25 Rozpucie, 26 Jabłonki

Three to eight petioles of each tree species were used to isolate the *P. fraxinina* cultures on 2% malt extract agar (MEA: 20 g L^{-1} malt extract, Difco, 15 g L^{-1} agar; Difco, Sparks, MD, USA), supplemented with 200 mg L^{-1} tetracycline (Tetracyclinum, TZF Polfa, Poland) in Petri dishes (diam. 9 cm). For this purpose, conidial mass collected from a single pycnidium was spread over the medium in the plate. After germination started, four to six small pieces of MEA with germinating conidia were excised and transferred onto 2% MEA in new Petri dishes. Morphology of colonies was examined in 28-day-old cultures grown on 2% MEA in darkness at 20 °C. Fragments of all the obtained cultures were transferred into Eppendorf tubes and are long-term stored at 4 °C (Table 2).

For comparison, our analyses included also other than *P. fraxinina* species of fungi that were detected on live and/or

dead ash petioles during our studies on ash decline. These species belonged to *Neocucurbitaria*, *Neopyrenochaeta* and *Pyrenochaeta* (Table 2). We also included five *Pyrenochaeta parasitica* (sexual morph *Nematostoma parasiticum*) strains (Table 2) that were obtained from needle browning symptomatic needles of *Abies alba* (Kowalski and Andruch 2012).

DNA extraction, PCR, and sequencing

Genomic DNA was extracted from 3-week-old, MEA-grown cultures using Genomic Mini AX Plant Kit (A&A Biotechnology, Gdynia, Poland) according to the manufacturer's protocol. Four loci, namely 18S–ITS1–5.8S–ITS2–28S (ITS rDNA), 28S (LSU rDNA), β-tubulin (*TUB2*), and RNA polymerase II second largest subunit (*RPB2*), were amplified for sequencing and phylogenetic analyses using the following primers: ITS5 and ITS4 for ITS rDNA (White et al. 1990), LR0R (Rehner and Samuels 1994), and LR5 (Vilgalys and Hester 1990) for LSU rDNA; T1HV and BtHV2r (Voglmayr et al. 2016) for *TUB2*; and RPB2-5F2 (Sung et al. 2007) and RPB2-P7R (Hansen et al. 2005) for *RPB2*. All four fragments were amplified in 25 µL reaction mixture containing 0.25 µL of Phusion High-Fidelity DNA polymerase (Finnzymes, Espoo, Finland), 5 µL of Phusion HF buffer (5×), 0.5 µL of dNTP mix (10 mM each), 0.75 µL of DMSO (100%), and 0.5 µL of each primer (25 µM). The reactions were run in a Biometra T-Personal 48 Thermocycler (Biometra GmbH, Goettingen, Germany) using the following cycling profile: an initial denaturation step at 98 °C for 30 s, followed by 35 cycles of 5 s at 98 °C, 10 s at 57 °C, and 30 s at 72 °C, and a final elongation at 72 °C for 8 min. The PCR products were visualized under UV light in 2% agarose gel stained with Midori Green (Nippon Genetic Europe).

Amplified products were sequenced bi-directionally using a BigDye® Terminator v 3.1 Cycle Sequencing Kit (Applied Biosystems, Foster City, CA, USA) and an ABI PRISM 3100 Genetic Analyzer (Applied Biosystems, Foster City, USA), at the DNA Research Centre (Poznań, Poland) with the use of PCR primers.

Sequence analyses

Obtained sequences were used as query in searches using the BLASTn (Altschul et al. 1990) algorithm to retrieve similar sequences from GenBank (http://www.ncbi.nlm.nih.gov). Accession numbers of these sequences are provided in Table 3.

The ITS-LSU rDNA fragments obtained from 21 isolates of *P. fraxinina* and from 15 related species were phylogenetically compared with ITS-LSU rDNA sequences of 88 representative species of *Pleosporales* (from GenBank) that allowed to determine taxonomic position of the species. The

protein coding *TUB2* and *RPB2* genes respectively for 28 and 22 strains were sequenced to enhance the delineation of closely related species (Table 2). Data sets for the concatenated ITS-LSU rDNA and ITS-LSU-*TUB2-RPB2* were used in phylogenetic analyses using *Massarina eburnea* and *Trematosphaeria pertusa* as outgroup.

Division into families and phylogenetic analyses were made according to data set provided by Jaklitsch et al. (2018). We excluded from these data the sequences of species phylogenetically remote to *P. fraxinina* and limited the number of OTUs for the same species. Data sets were compiled and edited with BioEdit v.2.7.5 (Hall 1999).

Both data sets were aligned with the online version of MAFFT ver. 7 (Katoh et al. 2019) using the following settings: the E-INS-i strategy with a 200PAM/κ=2 scoring matrix, a gap opening penalty of 1.53, and an offset value of 0.00. The alignments were checked manually with BioEdit v.2.7.5 (Hall 1999) and compared with gene maps (Yin et al. 2015) to ensure that introns and exons were aligned appropriately.

Phylogenetic analyses were performed individually, for each dataset, using three different methods: maximum likelihood (ML), maximum parsimony (MP), and Bayesian inference (BI). The best-fitted substitution models for each dataset were established for ML and BI using the corrected Akaike information criterion (AICc) in jModelTest 2.1.10 (Darriba et al. 2012; Guindon and Gascuel 2003).

ML analyses were conducted with PhyML 3.0 (Guindon et al. 2010) via the Montpelier online server (http://www.atgc-montpellier.fr/phyml/) using 1000 bootstrap pseudoreplicates to calculate node support values. The best evolutionary substitution model for ITS-LSU was GTR + I + G and for the combined ITS-LSU-*TUB2-RPB2* datasets was GTR + G.

MP analyses were conducted with PAUP* 4.0b10 (Swofford 2003). Gaps were treated as fifth state characters. One thousand bootstrap pseudoreplicates were generated and analyzed to determine the levels of confidence for the nodes within the inferred tree topologies. Tree bisection and reconnection (TBR) was selected as the branch swapping option. Tree length (TL), Consistency Index (CI), Retention Index (RI), Homoplasy Index (HI), and Rescaled Consistency Index (RC) were recorded for each dataset analyzed after the trees were generated. BI analyses based on a Markov chain Monte Carlo (MCMC) were carried out with MrBayes v3.1.2 (Ronquist and Huelsenbeck 2003). The MCMC chains were run for 10 million generations using the best-fit model for each data set. Trees were sampled every 100 generations, resulting in 100,000 trees from both runs. The default burn-in, first 25% of samples, was used. The remaining trees were utilized to generate a majority rule consensus tree and to determine the posterior probability node support values. The results of phylogenetic analyses were combined and visualized using TreeGraph 2.10.1-641 beta (Stöver and Müller 2010) and FigTree v1.4.0 (Rambaut 2006). All the alignments and trees

Table 2 Fungal isolates obtained in the present study

Species	Isolate number*	Host	Locality	Collection date	GenBank accession number		
					ITS-LSU	RPB2	TUB2
Nematostoma parasiticum	HMC 20345	*Abies alba*	Strzyżów	07.07.2012	MT547815	OM805995	MT547851
	HMC 20346	*Abies alba*	Strzyżów	07.07.2012	MT547816	OM805996	MT547852
	HMC 20347	*Abies alba*	Strzyżów	07.07.2012	MT547817	OM805997	MT547853
	HMC 20348	*Abies alba*	Strzyżów	10.07.2012	MT547818	OM805998	MT547854
	HMC 20351	*Abies alba*	Strzyżów	10.07.2012	MT547819	OM805999	MT547855
Neocucurbitaria quercina	281F	*Fraxinus pennsylvanica*	Jelcz	13.10.2017	MT547820	OM806000	MT547856
Neopyrenochaeta fragariae	282F	*Fraxinus pennsylvanica*	Jelcz	13.10.2017	MT547821	OM806001	MT547857
	462F	*Fraxinus excelsior*	Trzęsacz	17.10.2012	MT547822	OM806002	MT547858
	505F	*Fraxinus excelsior*	Dynów	26.08.2015	MT547823	OM806003	MT547859
Paracucurbitaria corni	10F	*Fraxinus excelsior*	Myślenice	12.09.2017	MT547824	OM806004	MT547860
	608F	*Fraxinus excelsior*	Miechów – Domiarki	26.08.2018	MT547825	not performed	not performed
	630F	*Fraxinus excelsior*	Miechów – Domiarki	26.08.2018	MT547826	not performed	MT547861
Pyrenochaeta fraxinina	43E*	*Acer pseudoplatanus*	Kowary	25.10.2014	MT547827	OM806005	MT547862
	44E	*Acer pseudoplatanus*	Kowary	07.10.2014	MT547828	not performed	not performed
	88E*	*Fraxinus excelsior*	Ojców	18.09.2013	MT547829	OM806006	not performed
	130E	*Fraxinus excelsior*	Myślenice	25.09.2013	MT547830	not performed	MT547863
	299E*	*Fraxinus mandshurica*	Rogów	11.10.2016	MT547831	not performed	MT547864
	454E*	*Fraxinus mandshurica*	Rogów	11.10.2016	MT547832	OM806007	MT547865
	456E*	*Fraxinus mandshurica*	Rogów	11.10.2016	MT547833	OM806008	MT547866
	187F*	*Fraxinus excelsior*	Brody	21.09.2017	MT547834	OM806009	MT547867
	278F*	*Fraxinus pennsylvanica*	Bystrzyca	03.10.2017	MT547835	OM806010	MT547868
	279F*	*Fraxinus pennsylvanica*	Bystrzyca	03.10.2017	MT547836	OM806011	MT547869
	280F*	*Fraxinus pennsylvanica*	Bystrzyca	03.10.2017	MT547837	OM806012	MT547870
	301F*	*Acer pseudoplatanus*	Brody	20.10.2017	MT547838	not performed	not performed
	504F	*Fraxinus excelsior*	Brody	28.10.2017	MT547839	not performed	MT547871
	530F	*Acer pseudoplatanus*	Myślenice	05.10.2018	MT547840	not performed	MT547872
	531F*	*Acer pseudoplatanus*	Ojców	05.10.2018	MT547841	not performed	MT547873
	532F	*Acer pseudoplatanus*	Brody	05.10.2018	MT547842	not performed	not performed
	533F	*Acer pseudoplatanus*	Brody	05.10.2018	MT547843	OM806013	MT547874
	743F*	*Fraxinus excelsior*	Jędrzejów	12.09.2018	MT547844	not performed	not performed
	746F	*Fraxinus excelsior*	Ojców	14.10.2018	MT547845	not performed	not performed
	747F	*Fraxinus excelsior*	Ojców	16.11.2018	MT547846	not performed	MT547875
	78F	*Fraxinus excelsior*	Brody	03.09.2017	MT547847	not performed	not performed
Pyrenochaeta sp. 1	724F	*Fraxinus pennsylvanica*	Brody	17.11.2018	MT547848	OM806014	MT547876
Pyrenochaeta sp. 2	79E	*Fraxinus excelsior*	Kowary	06.11.2014	MT547849	OM806015	MT547877
	321F	*Fraxinus excelsior*	Kowary	07.07.2014	MT547850	OM806016	MT547878

*Isolates used in temperature assay and in dual culture test with *Hymenoscyphus fraxineus*

generated in this study were deposited in TreeBASE (http://purl.org/phylo/treebase/phylows/study/TB2:S26391).

Newly obtained sequences were deposited in GenBank with accession numbers presented in Table 2.

Temperature assay

The temperature assay using twelve cultures, three for each host tree (Table 2), was carried out similarly to that performed for *Chalara fraxinea* by Kowalski and Bartnik (2010). Plugs (diam. 8 mm) from the edge of 21-day-old colonies actively growing on 2% MEA in darkness at 20 °C were transferred into new Petri dishes with 2% MEA and incubated at 5, 10, 15, 20, 25, 30, and 35 °C colony diameters (cm) were measured after 28 days. Two replicates were used for each combination; the average diameter from two measurements in each replicate was calculated. Effects of temperature on the

growth of *P. fraxinina* in vitro were analyzed with the Kruskal-Wallis test followed by nonparametric multiple comparison of mean ranks. All statistical calculations were performed using the STATISTICA software, version 10 (www.statsoft.com).

Antagonisms with *Hymenoscyphus fraxineus* in vitro

Twelve isolates of *P. fraxinina*, the same as previously used for temperature assay (Table 2), were screened by the in vitro dual culture assays on MEA for their ability to suppress the mycelial growth of *H. fraxineus*, the cause fungus of *F. excelsior* dieback. The *H. fraxineus* cultures Hf1 (=HMC 20952) and Hf2 (=HMC 21508) were isolated from the previous year's leaf petioles, with prominent pseudosclerotial plates of *H. fraxineus* (Bilański and Kowalski 2022). Plugs (diam. 8 mm) excised from 3-week-old cultures were placed at

a distance of 4 cm from each other on Petri dishes with MEA. After 21 days at 20 °C in the darkness, the interactions between the dual culture partners were assessed and growth measurements were taken. We considered two types of pathogen-saprotrophe interactions: (A) direct contact of the counterpart colonies without an inhibition zone, (B) occurrence of an inhibition zone. The inhibition of radial growth for both species was calculated according to the formula: (Rc - Ri)/Rc ×100, using mycelial growth toward counterpartner (Ri) and that on a control plate (Rc) as variables (Lahlali and Hijri 2010). The rate of mycelial growth reduction was estimated according to the following scale of colony radius reduction: (a) up to 25%; (b) 26–50%; (c) 51–75%; (d) > 75%; and (f) no growth inhibition. The inhibition zone width (mm) was measured along the axis joining the plugs used to inoculate the co-partners. The following four-step scale was used for the expression the width of the inhibition zone: Bs, up to 3 mm; Bm, between 4 and 5 mm; Bw, between 6 and 8 mm; and Bv, above 8 mm (see Bilański and Kowalski 2022).

Results

Occurrence and host spectrum

During the study, we documented the occurrence of *Pyrenochaeta fraxinina* pycnidial conidiomata on four deciduous tree species: *Fraxinus excelsior*, *F. mandshurica*, *F. pennsylvanica*, and *Acer pseudoplatanus* (Table 1). In the case of *F. excelsior*, the conidiomata occurred on 3.4% of the analyzed petioles (Table 1). The *P. fraxinina* occurrence on *F. excelsior* is widespread throughout Poland (Fig. 1); the fungus was detected in 17 out of 23 sampled forest sites (Table 1, Fig. 1). The occurrence was the most frequent at site No. 19 where it reached 15.4% of examined petioles (Fig. 1). Four additional sites (Nos. 1, 2, 11, 13) also proved to maintain relatively high *P. fraxinina* occurrence, the fruiting bodies were detected there on more than 10% of ash petioles (Fig. 1). For *F. pennsylvanica*, the *P. fraxinina* conidiomata occurred on 3.2% of analyzed petioles and were detected in all three sampling sites (Fig. 1). However, the occurrence on *F. mandshurica* petioles was more than twice less frequent (1.5%) and the conidiomata were observed only at single sampling site (Fig. 1). Pycnidia of *P. fraxinina* were also observed on 2.0% of examined *A. pseudoplatanus* petioles and were detected at 5 out of the overall 10 sampling sites where this species was sampled. The most frequent occurrence of *P. fraxinina* on *A. pseudoplatanus*, 8.3% of petioles, was recorded at site No. 19, the same site for which the occurrence on *F. excelsior* was the most common (Fig. 1). A relatively high frequency of *P. fraxinina* on *F. excelsior* was found in stands of approx. 25 to 60 years old (plots no. 1, 2, 6, 7, 11, 13, 19), growing on fresh (no. 1, 2, 11) or moist (no. 6, 7, 13, 19)

habitats, located both in the lowlands (no. 1, 2, 6, 7, 11) and highlands (no. 13, 19) (Fig. 1). Seasonal data compiled in Table 1 clearly show that *P. fraxinina* pycnidia in Poland are produced primarily in autumn and only occasionally in spring and summer.

The numbers of *P. fraxinina* pycnidia observed on a single petiole ranged from 1 to 31 and their position on a petiole varied (Fig. 2). Petioles of *F. excelsior* harbored separate pycnidia, single or in small clusters (Fig. 2a–c). They were produced on the surface (Fig. 2a) or under the epidermis being exposed only after the petiole's epidermis fractured longitudinally (Fig. 2c). In some instances, the longitudinal fracture resulted in separation of peripheral tissues of the petiole and their subsequent peeling off in form of strips. Consequently, *P. fraxinina* pycnidia become separated and carried away from the petioles along with these tissues (Fig. 2d, e). The pycnidia remaining on the petiole appeared as if they were formed not under the epidermis but on the petiole surface (Fig. 2f). Out of 93 *F. excelsior* petioles with *P. fraxinina* conidiomata, 26 (28.0%) petioles were colonized by *H. fraxineus* as well, evidenced by the characteristic black pseudosclerotial plate (Fig. 2g, h). For most of these petioles (24), *P. fraxinina* conidiomata were produced only within sections free of *H. fraxineus*. These were areas at the base of petioles (Fig. 2g), or sections distal from the base (Fig. 2h). Conidiomata of *P. fraxinina* formed directly on the *H. fraxineus* pseudosclerotial plate were observed only on 2 petioles (Fig. 2i). Pycnidia of *P. fraxinina* on *F. mandshurica* petioles occurred solitary on the petiole surface; no longitudinal epidermis fractures were observed (Fig. 2j). The pycnidia on *F. pennsylvanica* petioles occurred solitary or in clusters up to 6 (Fig. 2k). On *A. pseudoplatanus* petioles, the pycnidia were produced mostly on the surface, but occasionally also under the epidermis what caused its longitudinal fracture (Fig. 2l). Along with matured fruiting bodies of *P. fraxinina*, immature pycnidia were occasionally observed on ash and sycamore petioles (Fig. 2d–f, l).

Taxonomic treatment

Pyrenochaeta fraxinina Fairm.

Pycnidial conidiomata globose or slightly flatbed at the base, unilocular, pale-brown to brown-black, 210–600 μm in diameter, with single, central, circular ostiole 20–32 μm in diameter, non-papillate (Figs. 2a–l and 3a–g). Pycnidial wall of textura angularis, 15–22 μm thick, composed of cells 5–12 μm in diameter (Fig. 3a). Setae abundant around the ostiole and over the rest of the pycnidium (Fig. 2a–l), erect, dark brown, light brown in the apical part, thick-walled, unbranched, smooth, septate, tapered to the apices, with obtusely rounded end, 80–450 (600) μm long, 4–8 μm wide, widening

Table 3 Reference isolates and accession numbers included in the phylogenetic analyses

Taxon	Host/substrate	Strain	GenBank accession numbers			
			ITS	LSU	*RPB2*	*TUB2*
Allocucurbitaria botulispora	Human superficial tissue	CBS 142452	LT592932	LN907416	LT593070	LT593001
Alternaria alternata	*Arachis hypogaea*	CBS 916.96	KF465761	DQ678082	KC584375	–
Astragalicola amorpha	*Astragalus angustifolius*	CBS 142999	MF795753	MF795753	MF795795	MF795883
Coniothyrium palmarum	*Chamaerops humilispetioles*	CBS 400.71	AY720708	JX681084	DQ677956	KT389792
Cucitella opali	*Acer opalus*	CBS 142405	MF795754	MF795754	MF795796	MF795884
Cucurbitaria berberidis	*Berberis vulgaris*	CBS 130007	MF795758	MF795758	MF795800	–
Cucurbitaria berberidis	*Berberis vulgaris* ssp. *atropurpurea*	C39	MF795755	MF795755	MF795797	MF795885
Cucurbitaria berberidis	*Berberis* sp.	CBS 142401	MF795756	MF795756	MF795798	MF795886
Cucurbitaria oromediterranea	*Berberis cretica*	CBS 142399	MF795761	MF795761	MF795803	MF795890
Cucurbitaria oromediterranea	*Berberis aetnensis*	C265	MF795762	MF795762	MF795804	MF795891
Didymella exigua	*Rumex arifolius*	CBS 183.55	GU237794	EU754155	EU874850	GU237525
Dothidotthia symphoricarpi	*Symphoricarpos rotundifolius*	CBS 119687	–	EU673273	genome[a]	genome[a]
Fenestella fenestrata	*Alnus glutinosa*	CBS 143001	MF795765	MF795765	MF795807	MF795893
Leptosphaeria biglobosa	*Brassica napus*	G12-14	genome[b]	genome[b]	genome[b]	genome[b]
Leptosphaeria biglobosa	*Brassica oleracea*	CBS 476.81	MH861367	JX681092	–	–
Leptosphaeria doliolum	*Urtica dioica*	CBS 505.75	JF740205	GU301827	KT389640	JF740144
Leptosphaerulina australis	*Eugenia aromatica*	CBS 317.83	GU237829	GU301830	GU371790	GU237540
Leptosphaerulina nitida	*Alchemilla nitida*	CBS 450.84	MH861755	MH873454	–	–
Lizonia empirigonia	*Polytrichum commune*	CBS 542.76	genome[a]	genome[a]	genome[a]	genome[a]
Massarina eburnea	*Fagus sylvatica*	CBS 473.64	AF383959	GU301840	genome[a]	genome[a]
Nematostoma parasiticum	*Abies alba*	CBS 451.73	MH860737	GQ387617	–	–
Neocucurbitaria acanthocladae	*Genista acanthoclada*	CBS 142398	MF795766	MF795766	MF795808	MF795894
Neocucurbitaria acerina	*Acer pseudoplatanus*	C26a	MF795767	MF795767	MF795809	MF795895
Neocucurbitaria acerina	*Acer pseudoplatanus*	CBS 142403	MF795768	MF795768	MF795810	MF795896
Neocucurbitaria aetnensis	*Genista aetnensis*	CBS 142404	MF795769	MF795769	MF795811	MF795897
Neocucurbitaria aetnensis	*Genista aetnensis*	C270	MF795770	MF795770	MF795812	MF795898
Neocucurbitaria aquatica	Sea water	CBS 297.74	LT623221	EU754177	LT623278	LT623238
Neocucurbitaria cava	Unknown	CBS 115979	AY853248	EU754198	LT623273	LT623234
Neocucurbitaria cava	Wheat-field soil	CBS 257.68	JF740260	EU754199	LT717681	KT389844
Neocucurbitaria cinereae	*Genista cinerea*	CBS 142406	MF795771	MF795771	MF795813	MF795899
Neocucurbitaria cisticola	*Cistus monspeliensis*	CBS 142402	MF795772	MF795772	MF795814	MF795900
Neocucurbitaria hakeae	*Hakea* sp.	CBS 142109	KY173436	KY173526	KY173593	KY173613
Neocucurbitaria irregularis	Subcutaneous tissue	CBS 142791	LT592916	LN907372	LT593054	LT592985
Neocucurbitaria juglandicola	*Juglans regia*	CBS 142390	MF795773	MF795773	MF795815	MF795901
Neocucurbitaria keratinophila	Man corneal scrapings	CBS 121759	EU885415	LT623215	LT623275	LT623236
Neocucurbitaria populi	*Populus* sp.	CBS 142393	MF795774	MF795774	MF795816	MF795902
Neocucurbitaria quercina	*Quercus robur*	CBS 115095	LT623220	GQ387619	LT623277	LT623237
Neocucurbitaria rhamni	*Rhamnus frangula*	CBS 142391	MF795775	MF795775	MF795817	–
Neocucurbitaria rhamni	*Rhamnus frangula*	C112	MF795776	MF795776	MF795818	MF795903
Neocucurbitaria rhamni	*Rhamnus frangula*	C133	MF795777	MF795777	MF795819	MF795904
Neocucurbitaria rhamnicola	*Rhamnus lycioides*	CBS 142396	MF795780	MF795780	MF795822	MF795906
Neocucurbitaria rhamnicola	*Rhamnus alaternus*	KRx	MF795781	MF795781	MF795823	MF795907
Neocucurbitaria rhamnioides	*Rhamnus myrtifolius*	CBS 142395	MF795782	MF795782	MF795824	MF795908
Neocucurbitaria rhamnioides	*Rhamnus saxatilis* ssp. *prunifolius*	C222	MF795783	MF795783	MF795825	MF795909
Neocucurbitaria ribicola	*Ribes rubrum*	CBS 142394	MF795785	MF795785	MF795827	MF795911
Neocucurbitaria ribicola	*Ribes rubrum*	C155	MF795786	MF795786	MF795828	MF795912
Neocucurbitaria unguis-hominis	*Agapornis* sp. lung	CBS 111112	LT623222	GQ387623	LT623279	LT623239
Neocucurbitaria vachelliae	*Vachellia gummifera*	CBS 142397	MF795787	MF795787	MF795829	MF795913
Neopyrenochaeta acicola	Waterpipe	CBS 812.95	LT623218	GQ387602	LT623271	LT623232
Neopyrenochaeta fragariae	*Fragaria ananassa*	CBS 101634	LT623217	GQ387603	LT623270	LT623231
Neopyrenochaeta inflorescentiae	*Protea neriifolia*	CBS 119222	EU552153	EU552153	LT623272	LT623233
Neopyrenochaeta telephoni	Screen of a mobile phone	CBS 139022	KM516291	KM516290	LT717685	LT717678
Neopyrenochaetopsis hominis	Human superficial tissue	CBS 143033	LT592923	LN907381	LT593061	LT592992
Paracucurbitaria corni	*Fraxinus excelsior* with bacterial canker	CBS 248.79	LT903672	GQ387608	LT903673	LT900365
Paracucurbitaria italica	*Olea europaea*	CBS 234.92	LT623219	EU754176	LT623274	LT623235
Parafenestella mackenziei	*Rosa canina*	MFLUCC 16-1451	KY563071	KY563074	–	–
Parafenestella ostryae	*Ostrya carpinifolia*	MFLUCC 17-0097	KY563072	KY563075	–	–
Parafenestella pseudoplatani	*Acer pseudoplatanus*	CBS 142392	MF795788	MF795788	MF795830	MF795914
Phaeosphaeria ammophilae	*Ammophila arenaria*	AA	MF795789	MF795789	MF795831	–
Phaeosphaeriopsis glaucopunctata	*Ruscus aculeatus*	CBS 653.86	KF251199	KF251702	KF252206	KF252693
Phoma herbarum	*Rosa multiflora*	CBS 615.75	FJ427022	EU754186	KP330420	KF252703
Plenodomus hendersoniae	*Salix appendiculata*	LTO	MF795790	MF795790	MF795832	–
Protofenestella ulmi	*Ulmus minor*	CBS 143000	MF795791	MF795791	MF795833	MF795915

Table 3 (continued)

Taxon	Host/substrate	Strain	GenBank accession numbers			
			ITS	LSU	RPB2	TUB2
Pseudopyrenochaeta lycopersici	*Lycopersicon esculentum*	CBS 306.65	NR103581	EU754205	LT717680	LT717674
Pseudopyrenochaeta oryzae	*Oryza sativa*	CBS 110110	KF251186	KF251689	KF252193	KF252680
Pseudopyrenochaeta terrestris	Soil	CBS 282.72	LT623228	LT623216	LT623287	LT623246
Pyrenochaeta nobilis	*Laurus nobilis* leaf litter	CBS 407.76	MF795792	MF795792	MF795834	MF795916
Pyrenochaetopsis americana	Unknown	UTHSC DI16-225	LT592912	LN907368	LT593050	LT592981
Pyrenochaetopsis botulispora	Respiratory tract	CBS 142458	LT592946	LN907441	LT593085	LT593015
Pyrenochaetopsis confluens	Human blood	CBS 142459	LT592950	LN907446	LT593089	LT593019
Pyrenochaetopsis globosa	Human superficial tissue	CBS 143034	LT592934	LN907418	LT593072	LT593003
Pyrenochaetopsis leptospora	*Secale cereale*	CBS 101635	MF795793	MF795793	MF795835	MF795917
Pyrenochaetopsis uberiformis	Human superficial tissue	CBS 142461	LT592935	LN907420	LT593074	LT593004
Seltsamia ulmi	*Ulmus glabra*	CBS 143002	MF795794	MF795794	MF795836	MF795918
Staurosphaeria aptrootii	*Lycium* sp.	CBS 483.95	KY929149	GU301806	–	–
Trematosphaeria pertusa	*Fraxinus excelsior*	CBS 122368	AB809646	FJ201990	genome[a]	genome[a]
Xenopyrenochaetopsis pratorum	*Lolium perenne*	CBS 445.81	JF740263	GU238136	KT389671	KT389846

[a] Sequence retrieved from genome deposited at JGI-DOE (http://genome.jgi.doe.gov/)

[b] Sequence retrieved from genome deposited at GenBank (https://www.ncbi.nlm.nih.gov/assembly/GCA_900465125.1/)

at the basis to 9–14 (17) μm in diameter (Fig. 3g). Conidiophores filiform, branched at the base, hyaline, multiseptate, acropleurogenous, 40–75 (160) μm long, 1.5–4.0 μm wide, arose from the entire inner surface of the pycnidial wall (Fig. 3b–d). Conidiogenous cells enteroblastic, phialidic, in form of very short lateral branches immediately below transverse septa, with minute periclinal thickening (Fig. 3c–d). Conidia hyaline, golden olive in mass, smooth, aseptate, allantoid, occasionally straight or slightly curved 6.0–8.0 (10.0) × 1.0–1.5 μm, with 2 (rare 3–4) polar guttules (Fig. 3e, f). No sexual morph of *P. fraxinina* was observed on examined petioles.

Colonies reaching diameter of 3.9 to 5.4 cm after 4 weeks at 20 °C on MEA, smoky-gray, velutinous, smooth at the margin, slightly glistening, margin entire (Fig. 4a), rarely undulate or finely radially zonated. Reverse blackish-gray, foggy-gray at the center. Aerial mycelium hyphae hyaline to olive, little differentiated, diam. 1.5–3.0 μm, some hyphae joining to form bundles up to 15 μm thick. Substrate mycelium hyphae olive-brown, 1.8–3.5 μm in diam., with very frequent oil drops 0.6–1.8 μm in diam. Infrequent chlamydospore-like hyphal swollen cells up to 12 μm scattered throughout colonies. In vitro pycnidia or direct sporulation on the hyphae were not observed.

The microscopic features of the individual elements of the holotype (CUP-F No. 3368) determined from the analysis of one pycnidial conidioma were the following (Fig. 3h–k): Pycnidium globose, pale-brown, 220 μm in diam., with the basal part embedded in the substrate, central ostiole 30 μm in diam., non-papillate (Fig. 3i). Pycnidial wall of textura angularis, 16–20 μm thick, composed of cells 5–12 μm in diam. (Fig. 3i). Setae abundant, erect, dark brown, brighter at the top, thick-walled, unbranched, smooth, septate, blunt

ended, 90–300 μm long, 4–7 μm wide in the bottom part, basal cell 8–12 (14) μm in diam. (some setae in the bottom part were broken) (Fig. 3h–i). Conidiophores filiform, hyaline, multiseptate, branched at the base, acropleurogenous, 40–120 μm long, 2.0–4.0 μm wide. Conidia developed on short apical and lateral phialides immediately below transverse septa, hyaline, smooth, aseptate, allantoid, rarely straight or slightly curved 6.2–7.5 (10.0) × 1.2–1.5 μm, guttules only sporadically observed (Fig. 3j–k).

Representative cultures obtained from each tree species are deposited alive at the CBS Culture Collection, Utrecht, The Netherlands: CBS 146957 (from *A. pseudoplatanus*), CBS 146958 (*F. excelsior*), CBS 146959 (*F. pennsylvanica*) and CBS 146960 (*F. mandshurica*). The specimens examined are deposited in the Department of Forest Ecosystem Protection, University of Agriculture in Kraków, Poland. During the present research, two taxa, which could not be identified to the species level, were identified as *Pyrenochaeta* sp. 1 and *Pyrenochaeta* sp. 2 (Table 2). The first of them produced pycnidia on a single *F. pennsylvanica* petiole collected at site No. 18 (Fig. 1), which differed from typical *P. fraxinina* fruiting bodies mainly in that there was the lack of setae, but areas around ostiole and pycnidial wall were covered with thick-walled, smooth, olive-brown hair, irregularly twisted or coiled. *Pyrenochaeta* sp. 2 did not produce fruiting bodies, but was isolated from two previous year's petioles of *F. excelsior* collected from the litter at site No. 6 (Fig. 1).

Competition test in dual cultures

At the time of evaluation, in 58.3% of the dual cultures, there was a physical contact of the co-partners (Table 4, Fig. 4b). In the remaining cultures (41.7%), the formation of an inhibition
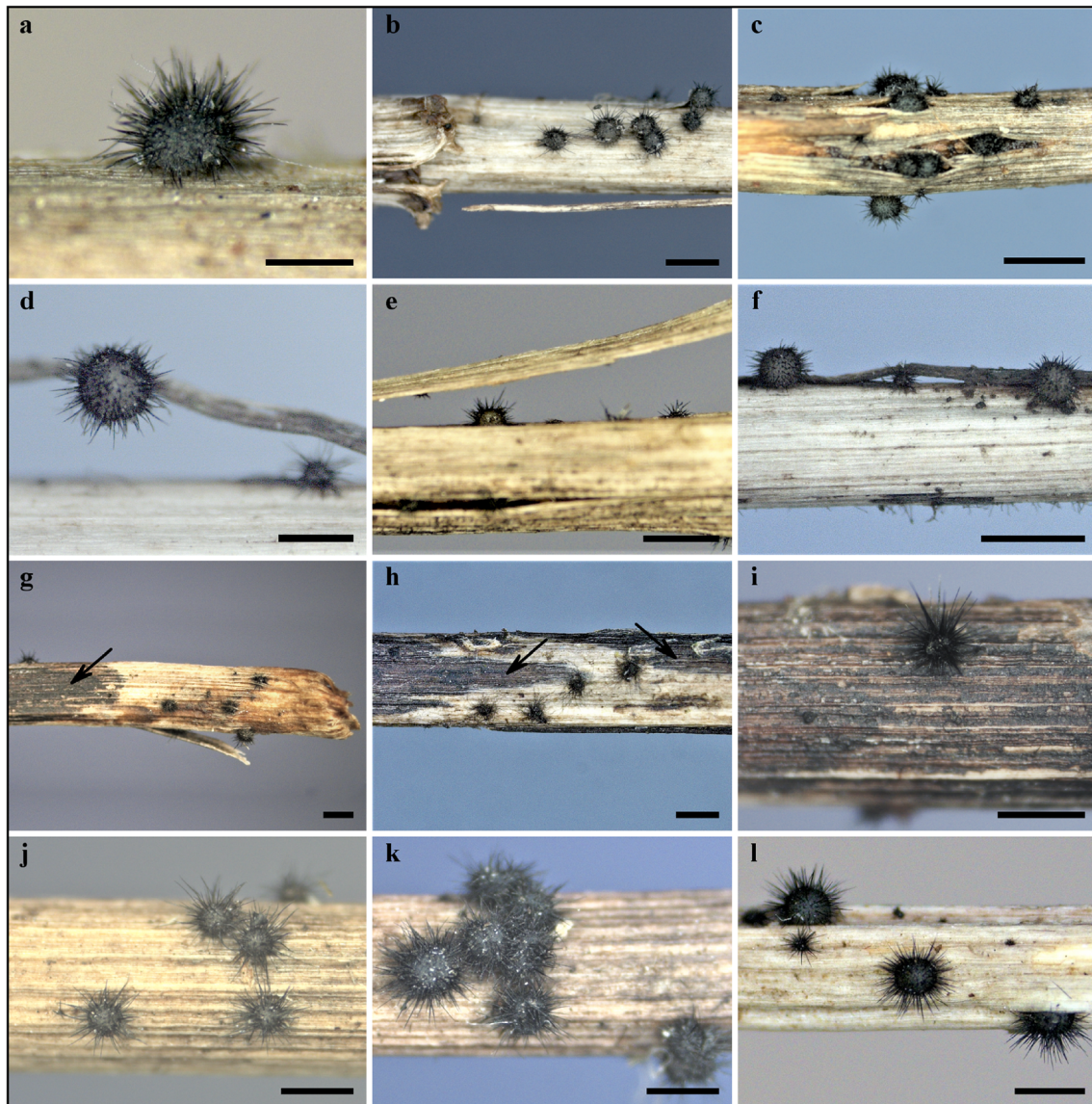
Fig. 2 Conidiomata of *Pyrenochaeta fraxinina* on ash and sycamore petioles in vivo. **a–i** Petioles of *F. excelsior*: **a, b** Solitary pycnidia on the petiole surface. **c** Pycnidia in groups within epidermis fracture. **d, e** Pycnidia separating from the petiole with stripes of peeling off epidermis. **f** Pycnidia remaining on petiole after epidermis peeled off. **g, h** Petiole colonized by *Hymenoscyphus fraxineus* with developed black pseudosclerotial plate (arrow) and bright fragments colonized by *P. fraxinina* (pycnidia) at the base of petiole (**g**) and at the distal part of petiole (**h**). **i** *P. fraxinina* pycnidium on black pseudosclerotial plate of *H. fraxineus*. **j** Solitary pycnidia of *P. fraxinina* on the surface of *F. mandshurica* petiole. **k** Clusters of pycnidia on the surface of *F. pennsylvanica* petiole. **l** *P. fraxinina* pycnidia at various development stages on petiole of *Acer pseudoplatanus*. – Bars: **a, d, j–l** = 0.5 mm; **b, c, e–i** = 1 mm

zone between co-partners (type B interaction) was observed (Table 4). In most cases, the width of the inhibition zone did not exceed 3 mm (type Bs) (Table 4, Fig. 4c). Only in three dual cultures the zone was wider and reached 4–5 mm (type Bm) (Table 4, Fig. 4d). Such wide zones were formed by isolates of *P. fraxinina* No. 43E and 88E (Table 2). In all the dual cultures, the radius (Ri) of both of *H. fraxineus* and *P. fraxinina* colonies was reduced, compared to that in the control (Rc). For most *H. fraxineus* cultures, this reduction was in the range of 26–50%, while for *P. fraxinina* 51–75% (Table 5).

Growth rate of *Pyrenochaeta fraxinina* at various temperatures

Colonies of *P. fraxinina* on MEA were able to grow at temperatures ranging from 5 to 25 °C (Fig. 5) regardless of their host origin. A single strain (454E) isolated from *F. mandshurica* was able to grow at 30 °C, the diameter of resulting colony did not differ statistically from some other isolates cultured at 5 and 10 °C (Fig. 5). No growth was observed at 35 °C for any isolate (Fig. 5). The optimal temperature was 20 °C but the differences in colony diameter at this
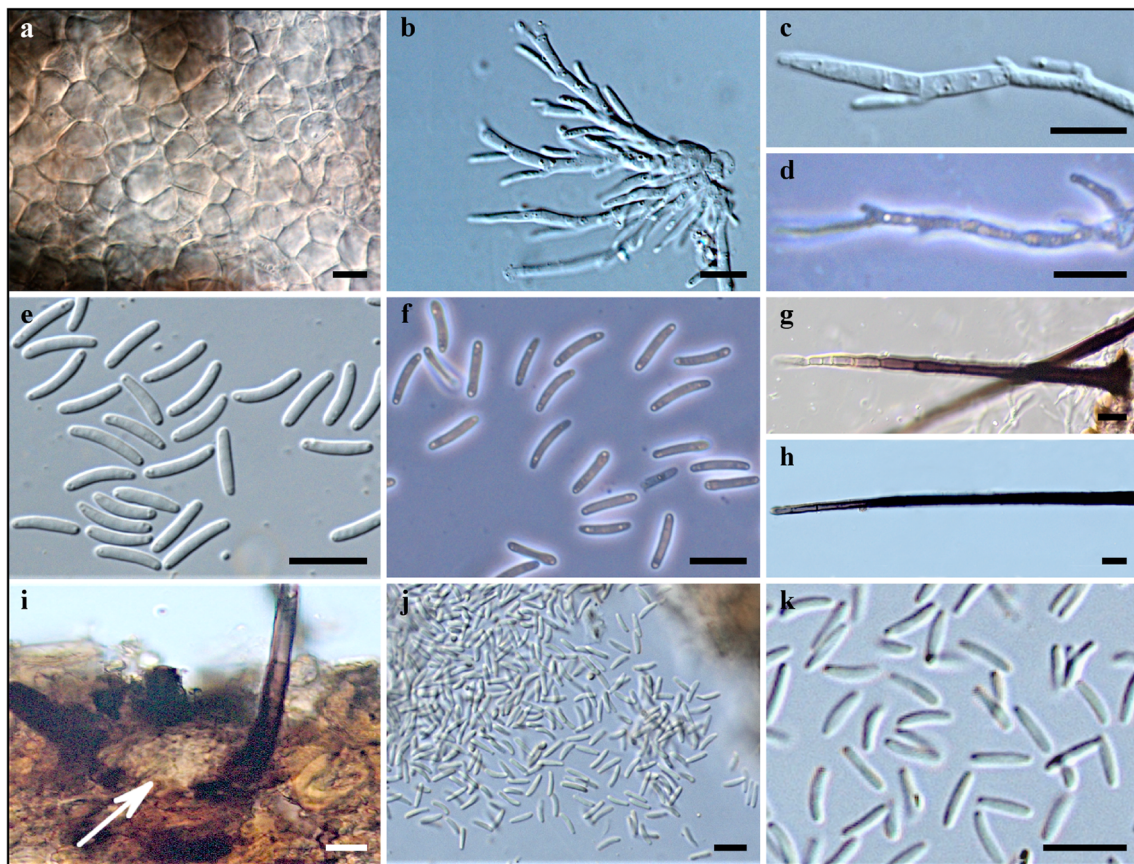
Fig. 3 Microstructures of *Pyrenochaeta fraxinina* conidiomata in vivo. **a**–**g** Polish samples: **a** Textura angularis of pycnidial wall. **b** Group of conidiophores with conidia. **c** Single conidiophore with conidia. **d** Single conidiophore with basal branch, phase-contrast. **e** Conidia from pycnidium on *F. excelsior* petiole. **f** Conidia from pycnidium on *F.* *mandshurica* petiole, phase-contrast. **g** Setae with septa and light brown apical part. **h**–**k** Holotype CUP-F. 3368: **h** Setae with septa and light brown apical part. **i** Pycnidial ostiole (arrow) and setae (some broken in basal part). **j**, **k** Conidia emerging from pycnidium. – Bars = 10 μm

temperature and at 15 and 25 °C (except for cultures isolated from *Acer pseudoplatanus*) were not statistically significant (Fig. 5). According to the Kruskal-Wallis test (α = 0.05), the temperatures 10, 15, and 25 °C did not have a statistically significant effect on the growth of *P. fraxinina* colonies in vitro (Fig. 5).

Phylogenetic analyses

Alignments for the ITS-LSU and the concatenated dataset of ITS-LSU-*TUB2-RPB2* contained respectively 1634 and 4326 characters (including gaps). The aligned *TUB2* gene region consisted of introns 1, 2, and 5 and exons 2, 3/4/ 5, 6, while lacking introns 3 and 4. The intron/exon arrangement of the *TUB2* for outgroup taxa, i.e., *Massarina eburnea* and *Trematosphaeria pertusa*, did contain, among others, introns 3 and 4.

In general, phylogenetic analysis using ITS-LSU sequences enabled species-level identification of isolates, e.g., diversity of this fragment was sufficient to distinguish *Paracucurbitaria corni* and *P. italica* (Fig. 6). In the resulting ITS-LSU tree, *P. fraxinina* clusters with *Nematostoma parasiticum*, *Pyrenochaeta* sp. 1, and *Pyrenochaeta* sp. 2 as well as with *Leptosphaerulina nitida* and *Staurosphaeria aptrootii* comprise a clear strongly supported lineage.

In both, ITS-LSU and ITS-LSU-*TUB2-RPB2* trees, all *P. fraxinina* strains form a clearly defined clade (Figs. 6 and 7), and there is no variation among *P. fraxinina* isolates resulting from their host origin (Figs. 6 and 7). Phylogenetically, *P. fraxinina* is closely allied to *Nematostoma parasiticum* (= *Herpotrichia parasitica,* asexual morph *Pyrenochaeta parasitica*) (Figs. 6 and 7). The concatenated ITS-LSU phylogeny also shows that Polish isolates of *N. parasiticum* did not differ from culture collection strain *N. parasiticum* CBS 451.73 (Fig. 6).

The analysis using ITS-LSU sequences was not sufficient to unequivocally define the family-level classification of species, as this phylogeny resulted in polyphyletic arrangements for the families (Fig. 6). The *P. fraxinina* lineage revealed in this analysis included, among others, *Leptosphaerulina nitida* and *Staurosphaeria aptrootii*, respectively members of *Didymellaceae* and *Coniothyriaceae* families. Monophyletic

Fig. 4 Colony of *Pyrenochaeta fraxinina* and interactions observed in dual cultures. **a** Colony of *P. fraxinina* (MEA, 4 weeks, 20 °C), **b–d** dual cultures of *P. fraxinina* (on the right) and *Hymenoscyphus fraxineus* (on the left) (MEA, 3 weeks, 20 °C): **b** direct contact of colonies without inhibition zone. **c** Inhibition zone–width type Bs (up to 3 mm). **d** Inhibition zone–width type Bm (4–5 mm). – Bars = 1 cm
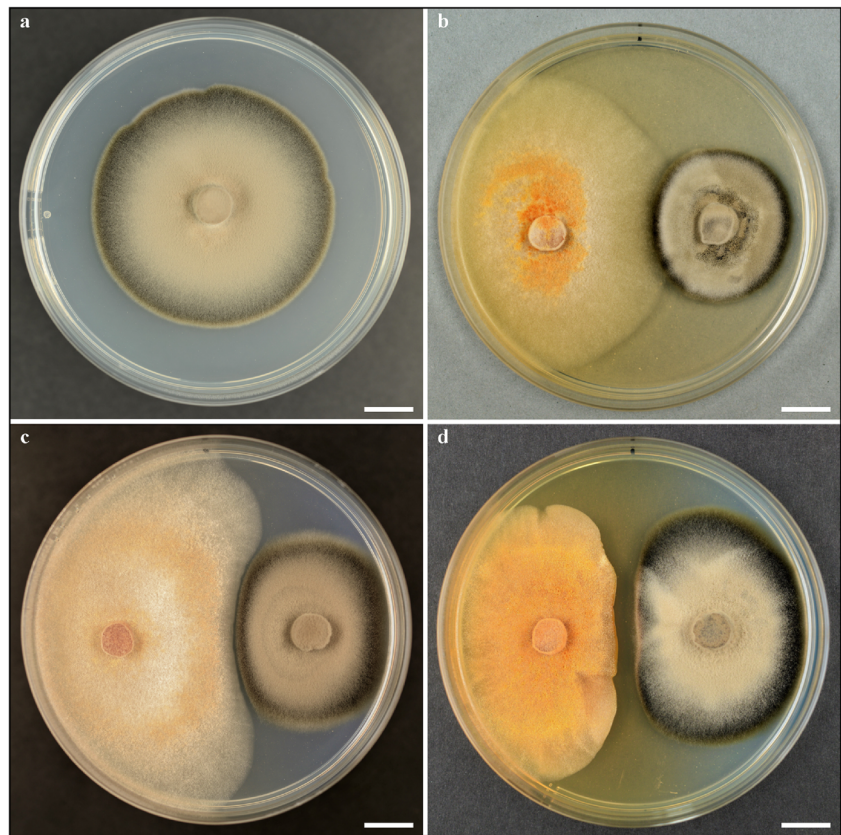
families were supported using ITS-LSU-*TUB2-RPB2* data (Fig. 7). According to this analysis, the *Leptosphaeriaceae* and *Coniothyriaceae* members were grouped outside the *P. fraxinina* clade.

Discussion

Occurrence and host spectrum

In this study, we documented the occurrence of *Pyrenochaeta fraxinina* on *Fraxinus excelsior*, *F. mandshurica*, *F. pennsylvanica*, and *Acer pseudoplatanus*. This is the new aspect of the fungus' host spectrum as the literature to date provides very little information in this regard. Even the original holotype description from USA lists only *Fraxinus* sp. petiole as substrate, the exact host species was not specified (Fairman 1913). Quite a different host species was reported by Schneider (1979) who, while analyzing an herbarium specimen from Hungary, identified *P. fraxinina* on withered stems of *Ruta graveolens*. The sample collected in 1957 by S. Tóth was originally identified as *Pyrenochaeta* sp. and this was the only European specimen of *P. fraxinina* analyzed in Schneider's (1979) monograph on the *Pyrenochaeta* genus. A condition that facilitated the *P. fraxinina* colonization of *A. pseudoplatanus* petioles may be its co-occurrence with *F.*

excelsior resulting in sycamore and European ash petioles lying intermixed in the forest floor. This indicates that sycamore petioles are suitable for *P. fraxinina* colonization as its conidiomata were not detected on petioles, or other leaf debris, of *Aesculus*, *Carpinus*, *Fagus*, or *Quercus* lying in the litter in the same conditions. This condition was different for *F. mandshurica* and *F. pennsylvanica* as, unlike *A. pseudoplatanus*, they always grew apart from *F. excelsior* stands. *Pyrenochaeta fraxinina* seems to show organ specificity to leaves; it was not detected on *F. excelsior* shoots with necrotic lesions, with no regard to how developed the lesions were (Przybył 2002; Bakys et al. 2009; Kowalski et al. 2016). One of the sites, where *P. fraxinina* on *F. pennsylvanica* was detected, was an urban greenery plot in Kraków-Zakrzówek, the same site on which the newly described *Hymenoscyphus pusillus* was recently identified on leaves of American green ash. This may indicate that this introduced ash species harbors an interesting spectrum of mycobiota yet to be fully identified (Kowalski and Bilański 2019).

Our results demonstrate that the occurrence of *P. fraxinina* in Poland is not local, and that the species is widespread in various regions of the country. However, most probably the habitat conditions at some sites particularly favor the *P. fraxinina* colonization of leaf residue in the litter resulting in relatively high, exceeding 10% of petioles, occurrence of the fungus. The exact numbers of colonized petioles may be in

Table 4 Interaction types in dual cultures between *Hymenoscyphus fraxineus* and *Pyrenochaeta fraxinina*

Interaction types	*Hymenoscyphus fraxineus* (strain) number (%)		
	Hf1	Hf2	Total
A (physical contact of mycelia)	8	6	14 (58.3)
B (inhibition zone) *	4	6	10 (41.7)
Number of dual cultures	12	12	24 (100.0)
* inhibition zone width			
Bs (up to 3 mm)	3	4	7
Bm (4–5 mm)	1	2	3
Bw (6–8 mm)	0	0	0
Bv (> 8 mm)	0	0	0

fact greater than recorded in our analyses, as according to our observations, the *P. fraxinina* conidiomata get detached from petioles with peeling off epidermis. A favorable condition for other *Pyrenochaeta* species on decomposing *Quercus* leaves was the rainy season (Rosales-Castillo et al. 2018). Another factor, which may play an important role in development of some *Pyrenochaeta*, is the temperature. For instance, the optimum growth temperature for *P. terrestris* is 25 or 27 °C, while for *P. lycopersici* it is 23 °C (Biles et al. 1992; Infantino et al. 2003). Both these species also produce microsclerotia that increase their ability to survive environmental extremes (Shishkoff and Campbell 1990; Biles et al. 1992). *Pyrenochaeta fraxinina* can grow in relatively broad range of temperatures, from 5 to 25 °C with optimum at 20 °C. This indicates that in Poland the fungus can actively colonize plant debris for a relatively long time each year, except for winter and for summer days with temperature exceeding 25 °C. Most probably *P. fraxinina* survives the adverse environmental conditions in pigmented hyphae in the substrate or in the chlamydospore-like structures that may function as resisting spores. The production of microsclerotia was not observed in vitro nor in vivo.

It is probable, that with the lack of *P. fraxinina* accessions available, the sequence-based identification would point to *Nematostoma parasiticum* (= *Herpotrichia parasitica*) as a species that proved to be the closest relative of *P. fraxinina* in our analyses. BLASTn searches (Altschul et al. 1990) using our

ITS sequences resulted in 97% or 98% similarity to *Herpotrichia* clone MDW-OTU-38 and in 95% similarity to *Herpotrichia parasitica* CBS 451.73. Such a situation can be found in the paper of Power et al. (2017) who while studying endophytes in branches of *F. excelsior* in New Zealand detected two species in the xylem and in the bark that were respectively 98% and 96% similar to *Herpotrichia parasitica*. These could be in fact *P. fraxinina*. If this information was confirmed, it would indicate the worldwide distribution of *P. fraxinina*.

Morphological aspects

Not all fungi producing setose pycnidia and hyaline conidia are classified in *Pyrenochaeta* but also in *Phoma* section *Paraphoma* (Boerema et al. 2004; de Gruyter et al. 2010). An important feature delimitating these two genera is the character of conidiogenesis. Apart from setose pycnidia, a feature characteristic to *Pyrenochaeta* is production of branched, filiform, septate, and acropleurogenous conidiophores (Schneider 1979; de Gruyter et al. 2010).

In general, the morphological characters of specimens analyzed in this study follow the descriptions of Fairman (1913) and Schneider's (1979) holotype analysis, the only difference concerns the size of conidiomata. Whereas Fairman (1913) specified their diameter as 220–330 μm, and Schneider (1979) as 220–350 μm, the petioles analyzed from Poland carried bigger conidiomata, the mature pycnidia were 210–

Table 5 Colony radius reduction of *Hymenoscyfus fraxineus* and *Pyrenochaeta fraxinina* in dual cultures

Reduction rate	*Hymenoscyphus fraxineus*			*Pyrenochaeta fraxinina*		
	Hf1	Hf2	Total number (%)	Hf1	Hf2	Total number (%)
a (< 25%)	1	0	1 (4.2)	0	0	0 (0.0)
b (26–50%)	10	7	17 (70.8)	6	3	9 (37.5)
c (51–75%)	1	5	6 (25.0)	6	9	15 (62.5)
d (> 75%)	0	0	0 (0.0)	0	0	0 (0.0)
f (0%)	0	0	0 (0,0)	0	0	0 (0.0)
Total	12	12	24 (100.0)	12	12	24 (100.0)
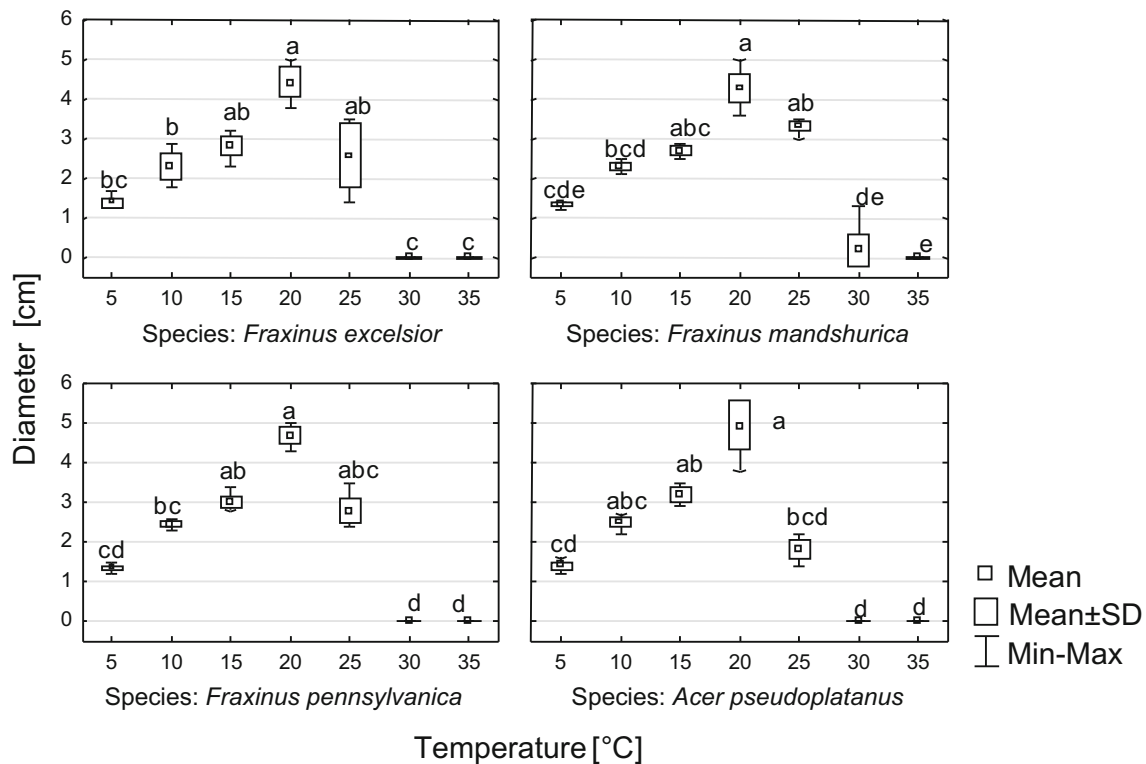
Fig. 5 Mean diameter of *Pyrenochaeta fraxinina* isolates from various host plants after 28 days growth at various temperatures. Values indicated with different letters in Kruskal-Wallis test are statistically significant at α = 0.05

600 μm in diameter. This difference may result from a greater number of analyzed samples or from the fact that we analyzed fresh material. Besides, we demonstrate that even a single petiole may carry conidiomata of various size, depending on their development stage (Fig. 2). In the currently analyzed holotype specimen, conidia only rarely contained the guttules. According to Baral (1989), despite the analysis of the old herbarium material, if spores are mounted in KOH, lipid bodies should be visible. Because Fairman (1913) gives "spores hyaline, granular" in original description, so this feature should be considered similar to that in Polish specimen.

A distinctive trait for *P. fraxinina* is allantoid conidia. Conidia of other *Pyrenochaeta* species are cylindrical, bilaterally rounded, straight, or only slightly curved (Schneider 1979). *Pyrenochaeta fraxinina* produces these conidia on long, filiform, acropleurogenous conidiophores, while for some *Pyrenochaeta* species the conidiophores are reduced to conidiogenous cells (Crous et al. 2014). Besides, *P. fraxinina* pycnidia have numerous long setae, both around ostiole as well as on the walls of the upper part of the pycnidium. For some other *Pyrenochaeta* species, the setae are located only around ostiole (Crous et al. 2014).

A level of morphological similarities exists between *P. fraxinina* and *P. parasitica* (sexual morph *Nematostoma parasiticum*). These include primarily features of conidiomata, which in *P. parasitica* are covered with dense dark-brown, 90–200-μm-long, setae around ostiole and along

the entire side walls of the pycnidia (Freyer and van der Aa 1975). The main difference between these two species concerns the morphology of conidia. These developed by *P. parasitica* are mostly cylindrical and much smaller, 4.2–5.2 × 1.3–2.3 μm (Freyer and Aa van der 1975). Another difference concerns the host spectrum. *Pyrenochaeta parasitica/ Nematostoma parasiticum* occurs on shoots and needles of silver fir (*Abies alba*) with the Herpotrichia needle browning (Freyer 1976; Butin 1995; Kowalski and Andruch 2012). Occasionally, it occurs also on *Picea* and *Tsuga* (Sivanesan 1984). So far, the species has been recorded in such European countries as Austria, Switzerland, Denmark, Germany, Norway, Great Britain, and Poland (Freyer and van der Aa 1975; Butin 1995; Kowalski and Andruch 2012) and sporadically in North America (Barr 1997). Our results show that petioles of *Fraxinus* spp. were also colonized by species with colonies or conidiomata morphologically very similar to *P. fraxinina*, which we provisionally designated as *Pyrenochaeta* sp.1 and *Pyrenochaeta* sp. 2. Proper identification of both taxons requires further study.

Phylogenetic positioning

The phylogenetic reconstructions using both, ITS-LSU and ITS-LSU-*TUB2-RPB2*, showed that *P. fraxinina* is distinct from other *Pleosporales* taxa. These analyses included also two undescribed *Pyrenochaeta* acquired in our study, both
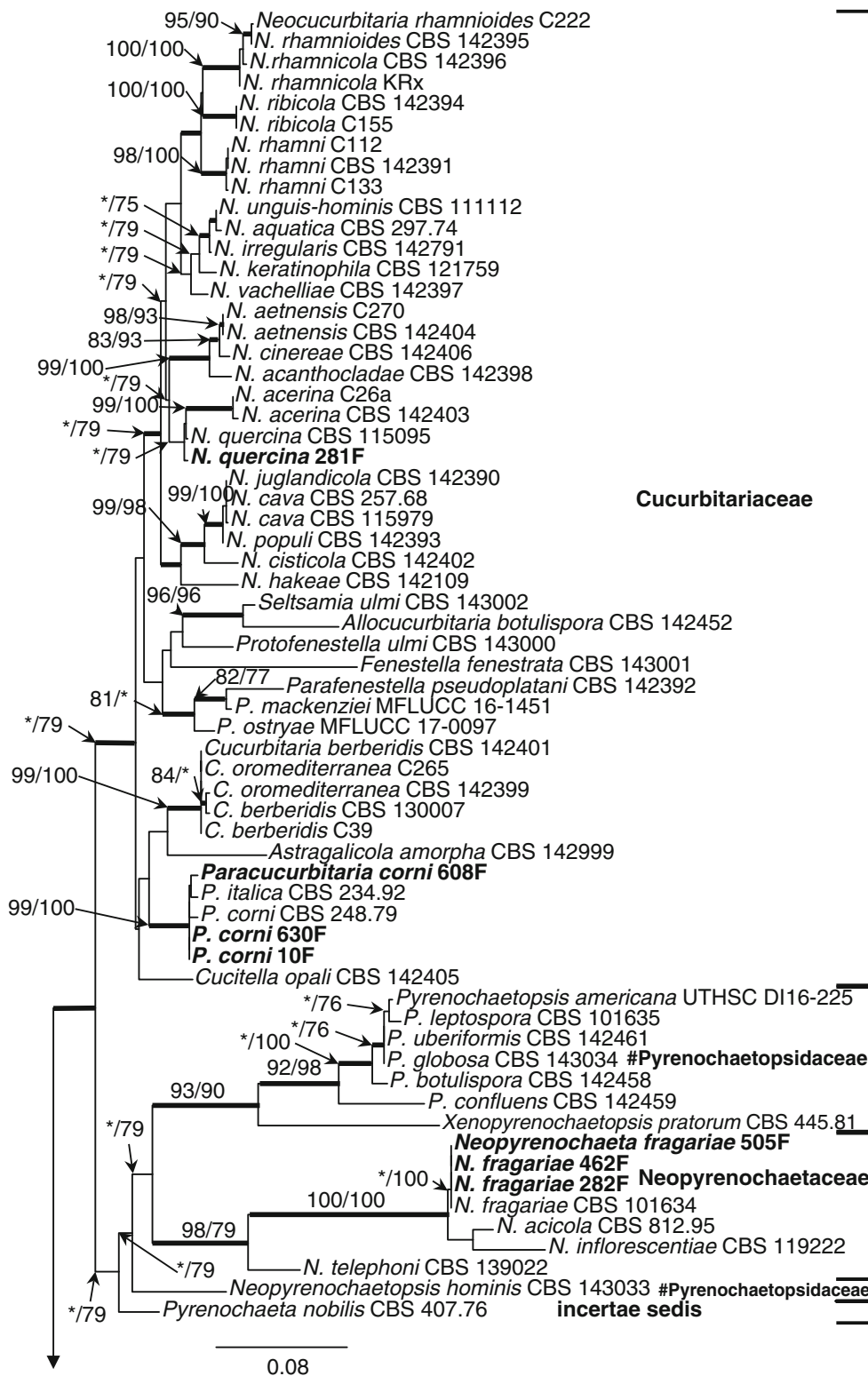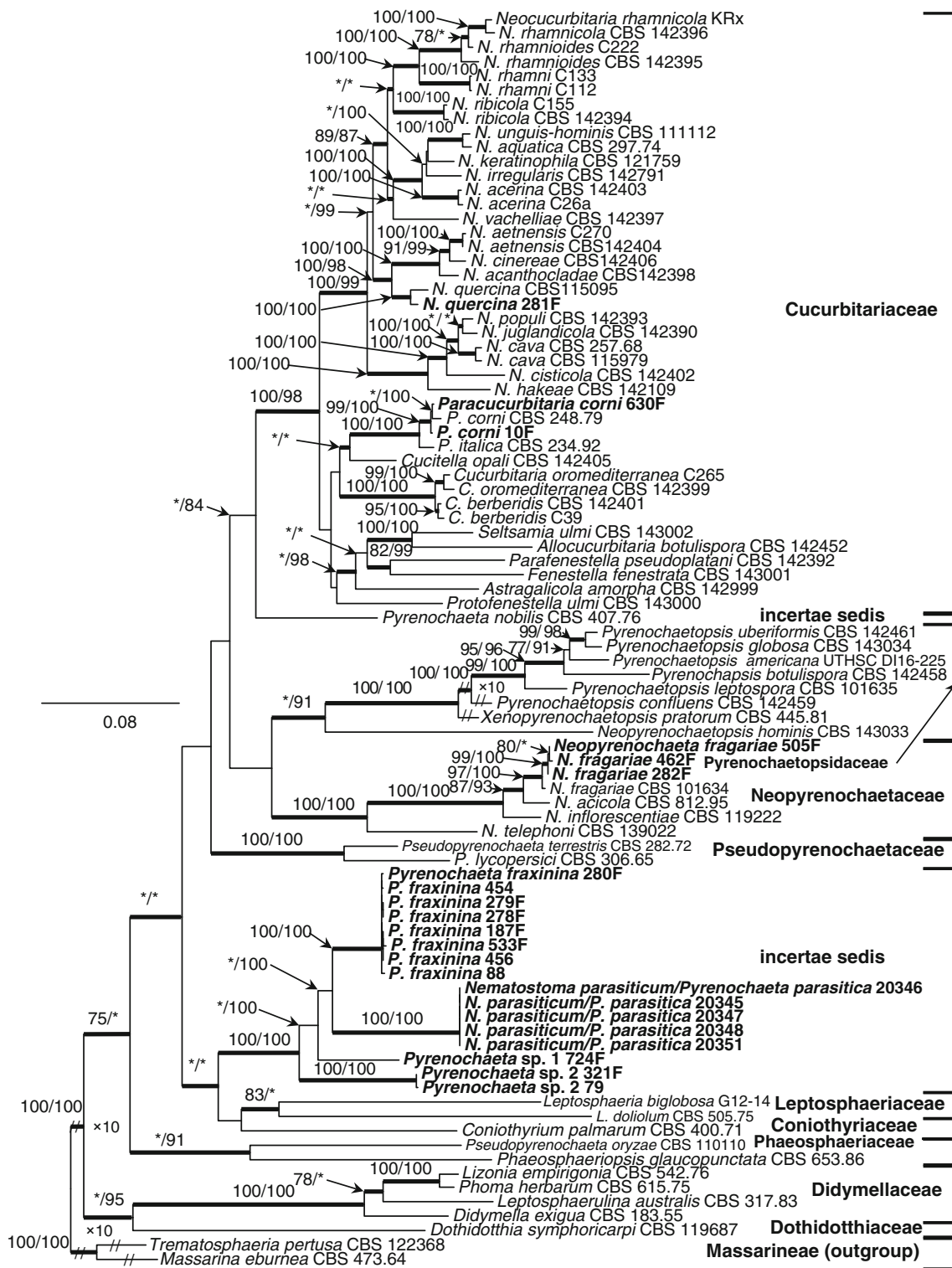
Fig. 6 Phylogram obtained from maximum likelihood (ML) analyses of the ITS-LSU for representative species and families of *Pleosporales*. Sequences obtained during this study are indicated in bold type. Bootstrap values ≥ 75% for ML and maximum parsimony (MP) analyses are presented at nodes (ML/MP). Bold branches indicate posterior probabilities values ≥ 0.95 obtained during Bayesian inference (BI) analyses. * indicate bootstrap values < 75%. The tree is drawn to scale (see bar) with branch length measured in the number of substitutions per site. *Massarina eburnea* and *Trematosphaeria pertusa* represent the outgroup in the analyses of ITS-LSU. # indicate polyphyletic family

Fig. 6 continued.

Pyrenochata sp. 1 and *Pyrenochaeta* sp. 2 were treated here as separate species. These results, along with other findings of this study, clearly showed that the diversity and taxonomic placement of many members of the *Pleosporales* are still poorly understood. However, the phylogenetic positioning of *P. fraxinina* showed its close relationship with *Nematostoma parasiticum* (= *Herpotrichia parasitica*, asexual morph *Pyrenochaeta parasitica*).

Pyrenochaeta fraxinina, *N. parasiticum*, *Pyrenochaeta* sp. 1, and *Pyrenochaeta* sp. 2 group into a strongly supported clade of undetermined family. Its sister clades group species

corresponding to families designated by Jaklitsch et al. (2018). This by comparison suggests that *P. fraxinina* clade also represents species of the same family. All the families of Jaklitsch et al. (2018) were reproduced as monophyletic clades in our ITS-LSU-*TUB2-RPB2* phylogeny, but the topology of this tree was different than the original tree of Jaklitsch et al. (2018) and tree of Valenzuela-Lopez et al. (2018). Thus, despite the clear result pointing to *Coniothyrium palmarum*, *Coniothyriaceae* member, as the closest relative of the *P. fraxinina* lineage, the relation to other families remains undetermined, as different analyses resulted in different branching

Fig. 7 Phylogram obtained from maximum likelihood (ML) analyses of the combined datasets of ITS-LSU-*TUB2-RPB2* for representative species and families of *Pleosporales*. Sequences obtained during this study are indicated in bold type. The Bootstrap values ≥ 75% for ML and maximum parsimony (MP) analyses are presented at nodes (ML/MP). Bold branches indicate posterior probabilities values ≥ 0.95 obtained during Bayesian inference (BI) analyses. * indicate bootstrap values < 75%. The tree is drawn to scale (see bar) with branch length measured in the number of substitutions per site. *Massarina eburnea* and *Trematosphaeria pertusa* represent the outgroup in the analyses of ITS-LSU-*TUB2-RPB2*

order of families' clades. Numerous papers, in which various *Pleosporales* have been included in phylogenetic analyses, propose different family level classifications of species within the order (Jaklitsch et al. 2018; Valenzuela-Lopez et al. 2018).

Pyrenochaeta and pyrenochaeta-like species, that are either independent species or are recognized asexual morphs of such well-known ascomycetous fungi as *Cucurbitaria*, *Herpotrichia*, *Nematostoma*, *Neopeckia*, *Byssosphaeria*, and *Keissleriella*, belong to different families within class *Dothideomycetes* (Lumbsch and Huhndorf 2010; Hyde et al. 2011; Wijayawardene et al. 2012, 2014; Doilom et al. 2013; Wanasinghe et al. 2017; Jaklitsch et al. 2018; Valenzuela-Lopez et al. 2018).

As reported by Hyde et al. (2011), *Nematostoma parasiticum* (as *Herpotrichia parasitica*) clusters basally in *Cucurbitariaceae*. According to other authors, *Nematostoma* is accepted as a genus with 13 species in *Pseudoperisporiaceae* family (Wijayawardene et al. 2017; Lumbsch and Huhndorf 2010; Hyde et al. 2011; Kirk et al. 2013). However, Wijayawardene et al. (2017) argues that these genera need revision, pointing to the fact that their cultures and sequences are unavailable. Based on our results, *P. fraxinina* and *N. parasiticum* are phylogenetically distant from the *Cucurbitariaceae* in terms proposed by Valenzuela-Lopez et al. (2018). Index Fungorum (2022) does not specify family for *P. fraxinina*, but only *Pleosporomycetidae* subclass of *Dothideomycetes*.

Hongsanan et al. (2020), analyzing the results of studies by other authors, found that phylogenetically, *Herpotrichia* is polyphyletic (Mugambi and Huhndorf 2009; Zhang et al. 2012; Tian et al. 2015; Hashimoto et al. 2017; Wanasinghe et al. 2018). Unfortunately, only a few works include *H. parasitica* in their phylogenetic analyzes (Crous et al. 2015; Tian et al. 2015). According to Crous et al. (2015), *H. parasitica* belongs to the *Pleosporaceae*. Tian et al. (2015) did not confirm the affiliation of *H. parasitica* to *Pleosporaceae*. According to Tian et al. (2015), *H. parasitica* formed a single clade located outside *Melanommataceae*. The results of the research conducted so far do not allow for certain classification of *Nematostoma parasiticum* to one of the known families.

For the correct taxonomic location of *P. fraxinina* and *N. parasiticum*, molecular studies of species within the genus *Nematostoma* are necessary. Moreover, there are indications that *P. fraxinina* should be transferred into the genus finally established for *N. parasiticum*.

Trophic aspects and interactions with *Hymenoscyphus fraxineus*

Some *Pyrenochaeta* species occur in ash tissues as endophytes; their colonization has been confirmed using molecular methods (Scholtysik et al. 2013; Haňáčková et al. 2017a; Ibrahim et al. 2017; Power et al. 2017; Bilański and Kowalski 2022). Until now, this group has not included *P. fraxinina*, which may results from the lack of *P. fraxinina* sequences deposited in the GenBank. The sequence data for 14 *P. fraxinina* strains generated in this study and submitted to GenBank should facilitate molecular identification of this species. Similarly, protein coding sequences for *P. parasitica* were not available in readily available sequence databases; the situation has been changed by submission of five sequences of *TUB2* and *RPB2* genes fragments that were generated in this study. These sequences would enable the more comprehensive phylogenetic analysis of *Pyrenochaeta sensu lato* in the future, and the correct delimitation of families and species.

On all ash and sycamore petioles analyzed in this study, *P. fraxinina* occurred saprotrophically in the litter. *Pyrenochaeta* spp. comprise an abundant group of litter decomposers also for other tree species (Voříšková and Baldrian 2013; Rosales-Castillo et al. 2018). Fungi involved in this process have been divided into various groups, depending on the time when they appear and on the level of decomposition of colonized leaves. According to this classification, *P. fraxinina* may be included to early decomposers (Frankland 1998; Rosales-Castillo et al. 2018). However presently, there is no information indicating the exact time when leaves get colonized by *P. fraxinina*. This is important not only as an aspect of succession in litter decomposition, but also as a factor affecting the ability of *P. fraxinina* to suppress the development of the ash dieback pathogen, *H. fraxineus*. Potentially, *P. fraxinina* may affect the inoculum buildup of *H. fraxineus* on European ash petioles. For most petioles, on which both *H. fraxineus* and *P. fraxinina* occurred together, they colonized separate petiole parts, which means that the presence of *P. fraxinina* reduces the availability of substrate for *H. fraxineus*. A particularly interesting situation (presented in Fig. 2g) occurs when *P. fraxinina* colonizes the base of the petiole. This means that *H. fraxineus* did not grow into the shoot before the leaf was dropped and was not able to cause shoot infection. This moment, i.e., crossing the leaf/shoot boundary, is one of the most important steps in development of ash dieback disease (Haňáčková et al. 2017b). The above observations correspond to the results of our in vitro analyses.

All dual cultures of *H. fraxineus* and *P. fraxinina* resulted in the growth inhibition of both fungi toward the counterpartner. The same situation was observed for most fungi when *H. fraxineus* was co-cultured with endophytic fungi isolated from European ash (Schulz et al. 2015; Haňáčková et al. 2017a; Bilański and Kowalski 2022). The inhibition by *H. fraxineus* could be due to the viridin

and a volatile lactone that the pathogen is known to produce (Grad et al. 2009; Andersson et al. 2012; Citron et al. 2014). The fact that in 41.7% of the combinations, the colony growth was suppressed without physical contact of mycelium may indicate that metabolites secreted into the medium play an important role in the interactions of studied fungi. Referring this to the in vivo situation, the separation of petiole sections colonized by *H. fraxineus* and *P. fraxinina* could be an effect of antibiosis or competition for substrate (Schulz and Boyle 2005; Hietala et al. 2018). The examples of growth suppression of *H. fraxineus* by *P. fraxinina* indicate that it may be an effective saprotrophic competitor in ash petioles. It cannot be ruled out that *P. fraxinina* has some mycoparasitic potential, as its conidiomata were sporadically produced directly on black pseudosclerotial plate of *H. fraxineus*. Recent studies suggest that the closest related to *P. fraxinina* species, *Nematostoma parasiticum*, can be a mycoparasite on *Rhizoctonia* sp. mycelium abundantly growing on dying needles and shoots of *Abies alba* (Kowalski and Andruch 2012; Butin 2014).

Data availability The data presented in this study are available in GenBank (https://www.ncbi.nlm.nih.gov).

Declarations

Ethics approval and consent to participate All authors confirm that no research involving humans or animals was involved in the current study, that there are no issues relating to animal welfare relating to the current study and that they have approval to participate in the current study.

Consent for publication All authors have given explicit consent to the submitted paper and to the inclusion of their data in it.

Competing interests The authors declare no competing interests.

References

Ahmed SA, van de Sande WWJ, Stevens DA et al (2014) Revision of agents of black-grain eumycetoma in the order *Pleosporales*. Persoonia - Mol Phylogeny Evol Fungi 33:141–154. https://doi.org/10.3767/003158514X684744

Altschul SF, Gish W, Miller W et al (1990) Basic local alignment search tool. J Mol Biol 215:403–410. https://doi.org/10.1016/S0022-2836(05)80360-2

Andersson PF, Bengtsson S, Stenlid J, Broberg A (2012) B-norsteroids from *Hymenoscyphus pseudoalbidus*. Molecules 17:7769–7781. https://doi.org/10.3390/molecules17077769

Bakys R, Vasaitis R, Barklund P et al (2009) Occurrence and pathogenicity of fungi in necrotic and non-symptomatic shoots of declining common ash (*Fraxinus excelsior*) in Sweden. Eur J For Res 128:51–60. https://doi.org/10.1007/s10342-008-0238-2

Baral H-O (1989) Contributions to the taxonomy of *Discomycetes* I. Zeitschrift für Mykol 55:119–130

Baral H-O, Bemmann M (2014) *Hymenoscyphus fraxineus* vs. *Hymenoscyphus albidus*—a comparative light microscopic study on the causal agent of European ash dieback and related foliicolous, stroma-forming species. Mycology 5:228–290. https://doi.org/10.1080/21501203.2014.963720

Baral H-O, Queloz V, Hosoya T (2014) *Hymenoscyphus fraxineus*, the correct scientific name for the fungus causing ash dieback in Europe. IMA Fungus 5:79–80. https://doi.org/10.5598/imafungus.2014.05.01.09

Barr ME (1984) *Herpotrichia* and its segregates. Mycotaxon 20:1–38

Barr ME (1997) Notes on some "dimeriaceous" fungi. Mycotaxon 64:149–171

Bates ST, Miller AN, the macrofungi collections and microfungi collections consortia (2018) The protochecklist of North American nonlichenized Fungi. Mycologia 110:1222–1348. https://doi.org/10.1080/00275514.2018.1515410

Bilański P, Kowalski T (2022) Fungal endophytes in *Fraxinus excelsior* petioles and their in vitro antagonistic potential against the ash dieback pathogen *Hymenoscyphus fraxineus*. Microbiol Res 257:126961. https://doi.org/10.1016/j.micres.2022.126961

Biles CL, Holland M, Ulloa-Godinez M et al (1992) *Pyrenochaeta terrestris* microsclerotia production and pigmentation on onion roots. HortSci 27:1213–1216. https://doi.org/10.21273/HORTSCI.27.11.1213

Boerema GH, de Gruyter J, Noordeloos ME, Hamers MEC (eds) (2004) *Phoma* identification manual. Differentiation of specific and infraspecific taxa in culture. CABI, Wallingford

Brambilla DP, Sutton BC (1969) Host index of species deposited in the mycological herbarium (WINF(M)) of the Forest Research Laboratory Winnipeg, Manitoba (February 1, 1969): Canadian

Forestry Service, Forest Research Laboratory Winnipeg, Manitoba. Intern Rep MS-90 1–104

Butin H (1995) Tree diseases and disorders: causes, biology and control in forest and amenity trees. Oxford University Press, Oxford

Butin H (2014) Die "Herpotrichia"-Nadelbräune der Tanne – Ein Irrtum und seine Berichtigung. Forstschutz Aktuell 59:12–14

Chen C, Hsieh W (2004) *Byssosphaeria* and *Herpotrichia* from Taiwan, with notes on the taxonomic relationship between these two genera. Sydowia 56:24–38

Citron CA, Junker C, Schulz B, Dickschat JS (2014) A volatile lactone of *Hymenoscyphus pseudoalbidus*, pathogen of european ash dieback, inhibits host germination. Angew Chem Int Ed 53:4346–4349. https://doi.org/10.1002/anie.201402290

Cleary M, Nguyen D, Marčiulynienė D et al (2016) Friend or foe? Biological and ecological traits of the European ash dieback pathogen *Hymenoscyphus fraxineus* in its native environment. Sci Rep 6: 21895. https://doi.org/10.1038/srep21895

Crous PW, Shivas RG, Quaedvlieg W et al (2014) Fungal planet description sheets: 214–280. Persoonia - Mol Phylogeny Evol Fungi 32: 184–306. https://doi.org/10.3767/003158514X682395

Crous PW, Wingfield MJ, Guarro J et al (2015) Fungal planet description sheets: 320–370. Persoonia - Mol Phylogeny Evol Fungi 34:167–266. https://doi.org/10.3767/003158515X688433

Darriba D, Taboada GL, Doallo R, Posada D (2012) jModelTest 2: more models, new heuristics and parallel computing. Nat Methods 9:772–772. https://doi.org/10.1038/nmeth.2109

de Gruyter J, Woudenberg JHC, Aveskamp MM et al (2010) Systematic reappraisal of species in *Phoma* section *Paraphoma*, *Pyrenochaeta* and *Pleurophoma*. Mycologia 102:1066–1081. https://doi.org/10.3852/09-240

de Gruyter J, Woudenberg JHC, Aveskamp MM et al (2013) Redisposition of *Phoma*-like anamorphs in *Pleosporales*. Stud Mycol 75:1–36. https://doi.org/10.3114/sim0004

De Notaris G (1849) *Micromycetes* Italici novi vel minus cogniti, decas 5. Mem della R Accad delle Sci di Torino Ser 2:333–350

Doilom M, Liu JK, Jaklitsch WM et al (2013) An outline of the family *Cucurbitariaceae*. Sydowia 65:167–192

Drenkhan R, Solheim H, Bogacheva A et al (2017) *Hymenoscyphus fraxineus* is a leaf pathogen of local *Fraxinus* species in the Russian Far East. Plant Pathol 66:490–500. https://doi.org/10.1111/ppa.12588

Enderle R, Stenlid J, Vasaitis R (2019) An overview of ash (*Fraxinus* spp.) and the ash dieback disease in Europe. CAB Rev 14:1–12. https://doi.org/10.1079/PAVSNNR201914025

Fairman CE (1913) Notes on new species of fungi from various localities. Mycologia 5:245–248. https://doi.org/10.1080/00275514.1913.12018524

Farr D, Bills G, Chamuris G, Rossman A (1989) Fungi on plants and plant products in the United States. APS Press, St. Paul

Frankland JC (1998) Fungal succession— unravelling the unpredictable. Mycol Res 102:1–15. https://doi.org/10.1017/S0953756297005364

Freyer K (1976) Untersuchungen zur Biologie, Morphologie und Verbreitung von *Herpotrichia parasitica* (Hartig) E. Rostrup (vormals *Trichosphaeria parasitica* Hartig). For Pathol 6:152–166. https://doi.org/10.1111/j.1439-0329.1976.tb00520.x

Freyer K, van der Aa HA (1975) Über *Pyrenochaeta parasitica* spec. nov., die Nebenfruchtform von *Herpotrichia parasitica* (Hartig) E. Rostrup (= *Trichosphaeria parasitica* Hartig). Eur J For Pathol 5: 177–182. https://doi.org/10.1111/j.1439-0329.1975.tb00463.x

Gargominy O (2019) TAXREF. Version 4.4. UMS PatriNat (AFB-CNRS-MNHN), Paris. Checklist dataset 10.15468/vqueam accessed via GBIF.org on 2019-12-14.

Grad B, Kowalski T, Kraj W (2009) Studies on secondary metabolite produced by *Chalara fraxinea* and its phytotoxic influence on *Fraxinus excelsior*. Phytopathologia 54:61–69

Gross A, Han JG (2015) *Hymenoscyphus fraxineus* and two new *Hymenoscyphus* species identified in Korea. Mycol Prog 14:19. https://doi.org/10.1007/s11557-015-1035-1

Gross A, Holdenrieder O (2013) On the longevity of *Hymenoscyphus pseudoalbidus* in petioles of *Fraxinus excelsior*. For Pathol 43: 168–170. https://doi.org/10.1111/efp.12022

Grove GG, Campbell RN (1987) Host range and survival in soil of *Pyrenochaeta lycopersici*. Plant Dis 71:806–809. https://doi.org/10.1094/PD-71-0806

Guindon S, Gascuel O (2003) A simple, fast and accurate method to estimate large phylogenies by maximum-likelihood. Syst Biol 52: 696–704. https://doi.org/10.1080/10635150390235520

Guindon S, Dufayard J-F, Lefort V et al (2010) New algorithms and methods to estimate maximum-likelihood phylogenies: Assessing the performance of PhyML 3.0. Syst Biol 59:307–321. https://doi.org/10.1093/sysbio/syq010

Hall TA (1999) BioEdit: a user-friendly biological sequence alignment editor and analysis program for Windows 95/98/ NT. Nucleic Acids Symp Ser 41:95–98

Haňáčková Z, Havrdová L, Černý K, et al (2017a) Fungal endophytes in ash shoots—diversity and inhibition of *Hymenoscyphus fraxineus*. Balt For 23:89–106

Haňáčková Z, Koukol O, Čmoková A et al (2017b) Direct evidence of *Hymenoscyphus fraxineus* infection pathway through the petiole-shoot junction. For Pathol 47:e12370. https://doi.org/10.1111/efp.12370

Hansen K, LoBuglio KF, Pfister DH (2005) Evolutionary relationships of the cup-fungus genus *Peziza* and *Pezizaceae* inferred from multiple nuclear genes: RPB2, β-tubulin, and LSU rDNA. Mol Phylogenet Evol 36:1–23. https://doi.org/10.1016/j.ympev.2005.03.010

Hashimoto A, Matsumura M, Hirayama K, Fujimoto R, Tanaka K (2017) *Pseudodidymellaceae* fam. nov.: phylogenetic affiliations of mycopappus-like genera in *Dothideomycetes*. Stud Mycol 87:187–206

Hietala AM, Børja I, Cross H et al (2018) Dieback of European ash: what can we learn from the microbial community and species-specific traits of endophytic fungi associated with ash? In: Pirttilä AM, Frank AC (eds) Endophytes of forest trees, Biology and applications, 2nd edn. Springer International Publishing, Cham, pp 229–258

Hongsanan S, Hyde KD, Phookamsak R, Wanasinghe DN et al (2020) Refined families of *Dothideomycetes*: Dothideomycetidae and Pleosporomycetidae. Mycosphere 11:1553–2107. https://doi.org/10.5943/mycosphere/11/1/13

Hyde K, McKenzie E, KoKo T (2011) Towards incorporating anamorphic fungi in a natural classification – checklist and notes for 2010. Mycosphere 2:1–88

Ibrahim M, Sieber TN, Schlegel M (2017) Communities of fungal endophytes in leaves of *Fraxinus ornus* are highly diverse. Fungal Ecol 29:10–19. https://doi.org/10.1016/j.funeco.2017.05.001

Index Fungorum (2022) http://www.indexfungorum.org. Accessed 2022 Feb 28

Infantino A, Aragona M, Brunetti A et al (2003) Molecular and physiological characterization of Italian isolates of *Pyrenochaeta lycopersici*. Mycol Res 107:707–716. https://doi.org/10.1017/S0953756203007962

Jaklitsch WM, Checa J, Blanco MN et al (2018) A preliminary account of the *Cucurbitariaceae*. Stud Mycol 90:71–118. https://doi.org/10.1016/j.simyco.2017.11.002

Katoh K, Rozewicki J, Yamada KD (2019) MAFFT online service: multiple sequence alignment, interactive sequence choice and visualization. Brief Bioinform 20:1160–1166. https://doi.org/10.1093/bib/bbx108

Kirk PM, Stalpers JA, Braun U et al (2013) A without-prejudice list of generic names of fungi for protection under the International Code

of Nomenclature for algae, fungi, and plants. IMA Fungus 4:381–443. https://doi.org/10.5598/imafungus.2013.04.02.17

Kowalski T (2006) *Chalara fraxinea* sp. nov. associated with dieback of ash (*Fraxinus excelsior*) in Poland. For Pathol 36:264–270. https://doi.org/10.1111/j.1439-0329.2006.00453.x

Kowalski T, Andruch K (2012) Mycobiota in needles of *Abies alba* with and without symptoms of Herpotrichia needle browning. For Pathol 42:183–190. https://doi.org/10.1111/j.1439-0329.2011.00738.x

Kowalski T, Bartnik C (2010) Morphologial variation in colonies of *Chalara fraxinea* isolated from ash (*Fraxinus excelsior* L.) stems with symptoms of dieback and effects of temperature on colony growth and structure. Acta Agrobot 63:99–106. https://doi.org/10.5586/aa.2010.012

Kowalski T, Bilański P (2019) *Hymenoscyphus pusillus*, a new species on leaves of *Fraxinus pennsylvanica* in Poland. For Pathol 49:e12481. https://doi.org/10.1111/efp.12481

Kowalski T, Bilański P (2021) Fungi detected in the previous year's leaf petioles of *Fraxinus excelsior* and their antagonistic potential against *Hymenoscyphus fraxineus*. Forests 12:1412. https://doi.org/10.3390/f12101412

Kowalski T, Kraj W, Bednarz B (2016) Fungi on stems and twigs in initial and advanced stages of dieback of European ash (*Fraxinus excelsior*) in Poland. Eur J For Res 135:565–579. https://doi.org/10.1007/s10342-016-0955-x

Læssøe T, Petersen JH, Heilmann-Clausen J, et al (2017) Danish Mycological Society - Checklist of Fungi. Version 1.8. Danish Mycological Society. Checklist dataset https://doi.org/10.15468/9zvguf Accessed via GBIF.org on 2019-12-27.

Lahlali R, Hijri M (2010) Screening, identification and evaluation of potential biocontrol fungal endophytes against *Rhizoctonia solani* AG3 on potato plants. FEMS Microbiol Lett 311:152–159. https://doi.org/10.1111/j.1574-6968.2010.02084.x

Lević J, Petrović T, Stanković S et al (2011) Frequency and incidence of *Pyrenochaeta terrestris* in root internodes of different maize hybrids. J Phytopathol 159:424–428. https://doi.org/10.1111/j.1439-0434.2011.01784.x

Lizoň P, Bacigalova K (1998) Fungi. In: Marhold K, Hindak F (eds) Checklist of nonvascular and vascular plants of Slovakia. Veda, Bratislava, pp 101–227

Lumbsch HT, Huhndorf SM (2010) Myconet Volume 14. Part One. Outline of *Ascomycota*—2009. Part Two. Notes on Ascomycete Systematics. Nos. 4751–5113. Fieldiana Life Earth Sci 1:1–64. https://doi.org/10.3158/1557.1

Mugambi GK, Huhndorf SM (2009) Molecular phylogenetics of *Pleosporales*: *Melanommataceae* and *Lophiostomataceae* recircumscribed (*Pleosporomycetidae*, *Dothideomycetes*, *Ascomycota*). Stud Mycol 64:103–121. https://doi.org/10.3114/sim.2009.64.05

Power M, Hopkins A, Chen J et al (2017) European *Fraxinus* species introduced into New Zealand retain many of their native endophytic fungi. Balt For 23:74–81

Przybyl K (2002) Fungi associated with necrotic apical parts of *Fraxinus excelsior* shoots. For Pathol 32:387–394. https://doi.org/10.1046/j.1439-0329.2002.00301.x

Rambaut A (2006) FigTree. Tree figure drawing tool version 1.4.0. Inst. Evol. Biol. Univ. Edinburgh. Available from http://tree.bio.ed.ac.uk/software/figtree/

Rehner SA, Samuels GJ (1994) Taxonomy and phylogeny of *Gliocladium* analysed from nuclear large subunit ribosomal DNA sequences. Mycol Res 98:625–634. https://doi.org/10.1016/S0953-7562(09)80409-7

Ronquist F, Huelsenbeck JP (2003) MrBayes 3: Bayesian phylogenetic inference under mixed models. Bioinformatics 19:1572–1574. https://doi.org/10.1093/bioinformatics/btg180

Rosales-Castillo J, Oyama K, Vázquez-Garcidueñas M et al (2018) Fungal community and ligninolytic enzyme activities in *Quercus*

deserticola Trel. Litter from forest fragments with increasing levels of disturbance. Forests 9(11). https://doi.org/10.3390/f9010011

Schlegel M, Queloz V, Sieber TN (2018) The endophytic mycobiome of European ash and sycamore maple leaves – geographic patterns, host specificity and influence of ash dieback. Front Microbiol 9. https://doi.org/10.3389/fmicb.2018.02345

Schneider R (1979) Die Gattung *Pyrenochaeta* De Notaris. Mitteilungen aus der Biol Bundesanstalt für Land- und Forstwirtschaft Berlin-Dahlem 189:1–73

Schoch CL, Shoemaker RA, Seifert KA et al (2006) A multigene phylogeny of the *Dothideomycetes* using four nuclear loci. Mycologia 98:1041–1052. https://doi.org/10.3852/mycologia.98.6.1041

Scholtysik A, Unterseher M, Otto P, Wirth C (2013) Spatio-temporal dynamics of endophyte diversity in the canopy of European ash (*Fraxinus excelsior*). Mycol Prog 12:291–304. https://doi.org/10.1007/s11557-012-0835-9

Schulz B, Boyle C (2005) The endophytic continuum. Mycol Res 109: 661–686. https://doi.org/10.1017/S095375620500273X

Schulz B, Haas S, Junker C et al (2015) Fungal endophytes are involved in multiple balanced antagonisms. Curr Sci 109:39–45

Shishkoff N, Campbell RN (1990) Survival of *Pyrenochaeta lycopersici* and the influence of temperature and cultivar resistance on the development of corky root of tomato. Plant Dis 74:889–894. https://doi.org/10.1094/PD-74-0889

Sieber TN (1995) *Pyrenochaeta ligni-putridi* sp. nov., a new coelomycete associated with butt rot of *Picea abies* in Switzerland. Mycol Res 99:274–276. https://doi.org/10.1016/S0953-7562(09)80897-6

Sinclair W, Lyon H (2005) Diseases of trees and shrubs, 2nd edn. Cornell University Press, Ithaca

Sivanesan A (1984) The bitunicate *Ascomycetes* and their anamorphs. J. Cramer, Vaduz

Stöver BC, Müller KF (2010) TreeGraph 2: Combining and visualizing evidence from different phylogenetic analyses. BMC Bioinforma 11:7. https://doi.org/10.1186/1471-2105-11-7

Sung G-H, Sung J-M, Hywel-Jones NL, Spatafora JW (2007) A multigene phylogeny of *Clavicipitaceae* (*Ascomycota*, Fungi): identification of localized incongruence using a combinational bootstrap approach. Mol Phylogenet Evol 44:1204–1223. https://doi.org/10.1016/j.ympev.2007.03.011

Sutton B (1980) The *Coelomycetes*. Fungi imperfecti with pycnidia, acervuli and stromata. Commonwealth Mycological Institute, Kew, Surrey, England

Swofford DL (2003) PAUP* 4.0. Phylogenetic analysis using parsimony (*and Other Methods). Sinauer Associates, Sunderland

Tian Q, Liu JK, Hyde KD et al (2015) Phylogenetic relationships and morphological reappraisal of *Melanommataceae* (*Pleosporales*). Fungal Divers 74:267–324. https://doi.org/10.1007/s13225-015-0350-9

Toh YF, Yew SM, Chan CL et al (2016) Genome anatomy of *Pyrenochaeta unguis-hominis* UM 256, a multidrug resistant strain isolated from skin scraping. PLoS One 11:e0162095. https://doi.org/10.1371/journal.pone.0162095

Valenzuela-Lopez N, Cano-Lira JF, Guarro J et al (2018) Coelomycetous *Dothideomycetes* with emphasis on the families *Cucurbitariaceae* and *Didymellaceae*. Stud Mycol 90:1–69. https://doi.org/10.1016/j.simyco.2017.11.003

Verkley GJM, Gené J, Guarro J et al (2010) *Pyrenochaeta keratinophila* sp. nov., isolated from an ocular infection in Spain. Rev Iberoam Micol 27:22–24. https://doi.org/10.1016/j.riam.2009.09.001

Vilgalys R, Hester M (1990) Rapid genetic identification and mapping of enzymatically amplified ribosomal DNA from several *Cryptococcus* species. J Bacteriol 172:4238–4246. https://doi.org/10.1128/jb.172.8.4238-4246.1990

Voglmayr H, Gardiennet A, Jaklitsch WM (2016) *Asterodiscus* and *Stigmatodiscus*, two new apothecial dothideomycete genera and

the new order *Stigmatodiscales*. Fungal Divers 80:271–284. https://doi.org/10.1007/s13225-016-0356-y

Voříšková J, Baldrian P (2013) Fungal community on decomposing leaf litter undergoes rapid successional changes. ISME J 7:477–486. https://doi.org/10.1038/ismej.2012.116

Wanasinghe D, Phookamsak R, Jeewon R et al (2017) A family level rDNA based phylogeny of *Cucurbitariaceae* and *Fenestellaceae* with descriptions of new *Fenestella* species and *Neocucurbitaria* gen. nov. Mycosphere 8:397–414. https://doi.org/10.5943/mycosphere/8/4/2

Wanasinghe DN, Phukhamsakda C, Hyde KD et al (2018) Fungal diversity notes 709–839: taxonomic and phylogenetic contributions to fungal taxa with an emphasis on fungi on *Rosaceae*. Fungal Divers 89:1–236. https://doi.org/10.1007/s13225-018-0395-7

White TJ, Bruns T, Lee S, Taylor JW (1990) Amplification and direct sequencing of fungal ribosomal RNA genes for phylogenetics. In: Innis MA, Gelfand DH, Sninsky JJ, White TJ (eds) PCR Protocols: A Guide to Methods and Applications. Academic Press Inc., New York, pp 315–322

Wijayawardene N, McKenzie E, Hyde K (2012) Towards incorporating anamorphic fungi in a natural classification – checklist and notes for 2011. Mycosphere 3:157–228. https://doi.org/10.5943/mycosphere/3/2/5

Wijayawardene NN, Crous PW, Kirk PM et al (2014) Naming and outline of *Dothideomycetes*–2014 including proposals for the protection or suppression of generic names. Fungal Divers 69:1–55. https://doi.org/10.1007/s13225-014-0309-2

Wijayawardene NN, Hyde KD, Rajeshkumar KC et al (2017) Notes for genera: *Ascomycota*. Fungal Divers 86:1–594. https://doi.org/10.1007/s13225-017-0386-0

Yang Y, Zuzak K, Harding M et al (2017) First report of pink root rot caused by *Setophoma* (*Pyrenochaeta*) *terrestris* on canola. Can J Plant Pathol 39:354–360. https://doi.org/10.1080/07060661.2017.1355849

Yin M, Duong TA, Wingfield MJ et al (2015) Taxonomy and phylogeny of the *Leptographium procerum* complex, including *Leptographium sinense* sp. nov. and *Leptographium longiconidiophorum* sp. nov. Antonie Van Leeuwenhoek 107:547–563. https://doi.org/10.1007/s10482-014-0351-9

Zhang Y, Crous PW, Schoch CL, Hyde KD (2012) *Pleosporales*. Fungal Divers 53:1–221. https://doi.org/10.1007/s13225-011-0117-x

Zhao Y-J, Hosoya T, Baral H-O et al (2013) *Hymenoscyphus pseudoalbidus*, the correct name for *Lambertella albida* reported from Japan. Mycotaxon 122:25–41. https://doi.org/10.5248/122.25

Zheng HD, Zhuang WY (2014) *Hymenoscyphus albidoides* sp. nov. and *H. pseudoalbidus* from China. Mycol Prog 13:625–638. https://doi.org/10.1007/s11557-013-0945-z